DEVELOPMENT OF THERMO-CHEMICAL MODEL AND EXERGETIC ASSESSMENT OF A BIOMASS DERIVED SYNGAS FUELED COMBINED CYCLE FOR COGENERATION OF POWER AND COOLING

BY

ROBHUL MIAH

A Thesis Presented to the
DEANSHIP OF GRADUATE STUDIES

KING FAHD UNIVERSITY OF PETROLEUM & MINERALS

DHAHRAN, SAUDI ARABIA

In Partial Fulfillment of the
Requirements for the Degree of

MASTER OF SCIENCE

In

MECHANICAL ENGINEERING

JANUARY 2017

KING FAHD UNIVERSITY OF PETROLEUM & MINERALS

DHAHRAN- 31261, SAUDI ARABIA

DEANSHIP OF GRADUATE STUDIES

This thesis, written by ROBHUL MIAH under the direction his thesis advisor and approved by his thesis committee, has been presented and accepted by the Dean of Graduate Studies, in partial fulfillment of the requirements for the degree of **MASTER OF SCIENCE IN MECHANICAL ENGINEERING.**

Dr. ABDUL KHALIQ
(Advisor)

Dr. ZUHAIR M. GASEM
Department Chairman

Dr. M. A. HABIB
(Member)

Dr. Salam A. Zummo
Dean of Graduate Studies

Dr. A. Z. SAHIN
(Member)

12/1/17
Date

Dedicated to

My Father, Mother and Sister whose prayer and inspiration brought me success in life

ACKNOWLEDGMENTS

All praises and thanks to Allah (s.w.t) for giving me the insight to carry out this work sincerely and complete my M.Sc. in Mechanical Engineering in King Fahd University of Petroleum and Minerals, Dhahran.

I would like to take the chance to express my gratitude toward Dr. Abdul Khaliq for his sagacious supervision. He taught me how to solve the hurdles of research works with steadfastness and perseverance. His problem specific directions with vast research expertise and continuous motivation make it possible to finish the work successfully.

I would like to thank all my committee members Dr. M.A. Habib and Dr. A.Z. Sahin for their insightful remarks of my thesis work. My deep gratitude to all the faculty members whom I interacted through the course works.

Last but not least, I am immensely indebted to my parents and sister for their endless love, prayer and psychological support.

TABLE OF CONTENTS

ACKNOWLEDGMENTS ..... **V**

TABLE OF CONTENTS ..... **VI**

LIST OF TABLES ..... **IX**

LIST OF FIGURES ..... **X**

LIST OF ABBREVIATIONS ..... **XIII**

ABSTRACT ..... **XVI**

ملخص الرسالة ..... **XVIII**

CHAPTER 1 INTRODUCTION **1**

1.1 Overview **1**

1.2 Gasification **3**

1.2.1 Main Stages of Gasification 3

1.2.2 Main Reactions Occur During Oxidation and Reduction in Gasifier 4

1.2.3 Types of Gasifiers 5

1.2.4 Gasifying Agents 6

1.2.5 Description of Various Models Utilized to Predict the Composition of Syngas 7

1.3 Integrated Gasification Combined Cycle (IGCC) **7**

1.4 LiBr-H_2O Absorption Cooling System **9**

CHAPTER 2 LITERATURE REVIEW **10**

2.1 Biomass Material **10**

2.2 Biomass Conversion to Energy (Waste to Energy) **10**

2.3 Syngas Utilization for Useful Energy Production **12**

2.4 Equilibrium model for a thermo-chemical gasification of biomass 13

2.5 Biomass Integrated Gasification Combined Cycle (BIGCC) for Power Generation 15

2.6 Syngas Utilization for Combined Power and Cooling production 16

2.7 Overall Objective of the Thesis 18

CHAPTER 3 SYSTEM DESCRIPTION AND METHODOLOGY 20

3.1 System Description 20

3.2 Methodology 22

3.3 Model Formulation 23

3.4 Thermodynamic Analysis 30

3.4.1 Energy Analysis 30

3.4.2 Exergy Analysis 31

3.5 Analysis of Individual Component of BIGCC 34

3.5.1 Compressor 34

3.5.2 Gasifier 34

3.5.3 Combustion chamber 36

3.5.4 Gas Turbine 36

3.5.5 Heat Recovery Steam Generator 37

3.5.6 Steam Turbine 38

3.5.7 Steam Condenser 39

3.5.8 Feed Pump 39

3.6 Absorption Refrigeration Cycle 40

3.6.1 Generator 42

3.6.2 Refrigerant Condenser 43

3.6.3 Expansion valve-1 43

3.6.4 Evaporator 44

3.6.5 Absorber 44
3.6.6 Solution pump 45
3.6.7 Solution heat exchanger 45
3.6.8 Exergy of LiBr-H_2O Solution 46

3.7 Energy and Exergy Efficiency of the Combined Power and Cooling Cycle 48

CHAPTER 4 RESULTS AND DISCUSSION 50

4.1 Effect of Change in Gasification Equivalence Ratio 50

4.2 Effect of Change in Steam to Biomass Ratio (SBR) 58

4.3 Effect of Change in Compressor Pressure Ratio 65

4.4 Effect of Change in Pinch Point Temperature at HRSG 72

4.5 Exergy Efficiency of Every Component 76

CHAPTER 5 CONCLUSION AND RECOMMENDATIONS 80

REFERENCES 83

VITAE 89

LIST OF TABLES

Table 1: Biomass properties..... 24

Table 2: The comparison of results of gas composition related to biomass with the data from researchers..... 28

Table 3: Chemical exergy of different elements..... 33

Table 4: Values of $\boldsymbol{aij}$ and $\boldsymbol{bij}$ 48

LIST OF FIGURES

Figure 1: Total energy consumption in the world[1] 1

Figure 2: Main stages of gasification 4

Figure 3: Updraft and downdraft gasifier 5

Figure 4: Bubbling bed and circulating bed gasifier 6

Figure 5: Schematic of a typical IGCC plant based on coal[6] 8

Figure 6: Schematic diagram of a biomass derived combine cycle power plant 20

Figure 7: BIGCC with LiBr-H_2O absorption refrigeration system 22

Figure 8: Basic principle of an air-steam biomass gasifier 24

Figure 9: Exergy in stages 31

Figure 10: Pinch point temperature in HRSG 37

Figure 11: Effect of gasification equivalence ratio on the LHV of producer gas 51

Figure 12: Effect of equivalence ratio on the energy efficiency of gasifier 52

Figure 13: Effect of equivalence ratio on the exergy efficiency of gasifier 53

Figure 14: Effect of gasification equivalence ratio on the energy efficiency of BIGCC . 55

Figure 15: Effect of gasification equivalence ratio on the exergy efficiency of BIGCC . 56

Figure 16: Effect of equivalence ratio in energy efficiency of BIGCC with LiBr-H_2O cooling system 57

Figure 17: Effect of equivalence ratio in Exergy Efficiency of BIGCC with LiBr-H_2O cooling system 58

Figure 18: Effect of SBR on the LHV of the producer gas 59

Figure 19: Effect of steam to biomass ratio on the energy efficiency of gasifier 60

Figure 20: Effect of steam to biomass ratio on the exergy efficiency of gasifier 61

Figure 21: Effect of steam to biomass ratio on the energy efficiency of BIGCC..... 62

Figure 22: Effect of steam to biomass ratio on the exergy efficiency of BIGCC..... 63

Figure 23: Effect of steam to biomass ratio in energy efficiency of BIGCC with LiBr-H_2O cooling system 64

Figure 24: Effect of steam to biomass ratio in exergy efficiency of BIGCC with LiBr-H_2O cooling system 65

Figure 25: Effect of compressor ratio on the LHV of producer gas 66

Figure 26: Effect of compressor pressure ratio on the energy efficiency of gasifier..... 67

Figure 27: Effect of compressor pressure ratio on the exergy efficiency of gasifier..... 68

Figure 28: Effect of compressor pressure ratio on the energy efficiency of BIGCC 69

Figure 29: Effect of compressor pressure ratio on the exergy efficiency of BIGCC 70

Figure 30: Effect of compressor pressure ratio in energy efficiency of BIGCC with LiBr-H_2O cooling system 71

Figure 31: Effect of compressor pressure ratio in exergy efficiency of BIGCC with LiBr-H_2O cooling system 72

Figure 32: Effect of pinch point temperature at HRSG on the energy efficiency of BIGCC 73

Figure 33: Effect of pinch point temperature at HRSG on the exergy efficiency of BIGCC 74

Figure 34: Effect of pinch point in HRSG in energy efficiency of BIGCC with LiBr-H_2O cooling system 75

Figure 35: Effect of pinch point of HRSG in exergy efficiency of BIGCC with LiBr-H_2O cooling system 76

Figure 36: Exergy efficiency of the components of the BIGCC at mean operating condition 77
Figure 37: Exergy efficiency of each component with physical exergy in VAR 78
Figure 38: Exergy efficiency of every component with physical and chemical exergy in VAR 79

LIST OF ABBREVIATIONS

$\bar{h}_{f_i}^{o}$	Formation Enthalpy of species i (kJ/kmol)
$\bar{C}_{p_i}$	Specific Heat (kJ/kmol-K)
$\bar{R}$	Universal Gas Constant (kJ/kmol–K)
a_{H_2O}	Activity of H_2O
a_{LiBr}	Activity of LiBr
a_i, b_i	Co-efficient in Eqs. 101-104
a, b	Mole Numbers (kmol) in Eqs. 1-40
BIGCC	Biogas Integrated Gasification Combined Cycle
e	Specific Exergy (kJ/kmol)
E	Exergy (kJ)
ex	Chemical Exergy in LiBr-H_2O Solution
GER	Gasification Equivalence Ratio
h	Specific Enthalpy (kJ/kmol)
H	Energy Content (kJ)
HRSG	Heat Recovery Steam Generator
k	Equilibrium Constant
LHV	Lower Heating Value
LiBr	Lithium Bromide
m	Mass (kg) and Molality in Eqs. 100 to 105
M	Molecular Weight (kg/kmol)
n	Mole Number (kmol)
PP	Pinch Point (K)
Q_j	Heat Transfer (kJ)

s	Specific Entropy (kJ/kmol-K)
SBR	Steam to Biomass Ratio (kg/kg)
SFR	Steam to Fuel Ratio (kmol/kmol)
SHE	Solution Heat Exchanger
T	Temperature (K)
VAR	Vapor Absorption Refrigeration
W	Work Done (kJ)
y_i	Mole Fraction of 'I'
x	Mass Fraction of LiBr in LiBr-H_2O Solution
$\Delta\bar{h}_i$	Change of Enthalpy of species 'I' (kJ/kmol)

Greek Letters

α	Carbon Conversion Factor
η	Efficiency
ϕ	Osmotic Co-efficient

Subscripts

1-32	Points in BIGCC-VAR
a,b,c,d	Points in HRSG
abs	Absorber
bio	Biomass
c	Compressor
cc	Combustion Chamber
ch	Chemical
ch,dest	Destruction of Chemical Exergy

ch,o	Standard Chemical Exergy
D	Destruction
evap	Evaporator
ex	Expansion
fp	Feed Pump
g	Gasifier
gasi	Gasifier
gen	Generator
gt	Gas Turbine
ph	Physical
r	Refrigerant
ref,cond	Refrigerant Condenser
SHE	Solution Heat Exchanger
sol	Solution of LiBr-H_2O
sp	Solution Pump
ss	Strong Solution
st	Steam Turbine
stm,cond	Steam Condenser
syn	Syngas
ws	Weak Solution

ABSTRACT

Full Name : [Robhul Miah]

Thesis Title : Development of thermo-chemical model and exergetic assessment of a biomass-derived syngas fueled combined cycle for cogeneration of power and cooling

Major Field : [Mechanical Engineering]

Date of Degree : [January 2017]

Among all the renewable sources of energy, biomass has been found as the most promising one due to its abundant availability and CO_2 neutral nature. The efficient and environmentally benign method for its conversion to the valuable gaseous product is gasification which is a thermo-chemical method. In this regard, the present study was aimed to develop a generalized thermo-chemical model for the conversion of biomass material to useful gaseous fuel called syngas. The model developed incorporated the phenomena of char conversion, tar formation and thermodynamic equilibrium concept, which can compute the composition of syngas. The effects of change in the operating variables like; compressor pressure ratio, gasification equivalence ratio (GER), steam-biomass ratio (SBR), and pinch point of HRSG were examined on the performance parameters of BIGCC, and combined BIGCC-VAR cycle, like the energy and exergy efficiency of BIGCC, and combined cycle. It has been found that at low values of gasification equivalence ratio the LHV of syngas as well as the energy and exergy efficiency of the gasifier are high for all biomass materials. The effect of GER on the energy and exergy efficiencies of BIGCC is more pronounced at higher values of GER. Both energy and exergy efficiencies of the gasifier decrease with increase in SBR but the

energy and exergy efficiencies of BIGCC increases as the SBR increases. The energy and exergy efficiency of BIGCC increases with the increase in the gasifier pressure and decreases with the increase in the pinch point temperature of HRSG. Employment of LiBr-H_2O absorption refrigeration system at the exit of HRSG show an improvement in both the energy and exergy efficiency of the BIGCC. The inclusion of the chemical exergy of LiBr-H_2O along with the physical exergy show very interesting results and these results clearly reveal that computations made after taking into account the chemical exergy widely change the exergy efficiency of the major components of the proposed combined power and cooling cycle.

ملخص الرسالة

الاسم الكامل: ربهول ميا

عنوان الرسالة: تطوير نموذج حراري-كيميائي وتقييم إكسرجي لوقود الغاز المتزايد المستخلص من الكتلة الحيوية لتغذية الدورة المركبة من التوليد المشترك للطاقة و التبريد.

التخصص: الهندسة الميكانيكية

تاريخ الدرجة العلمية: يناير 2017

من بين جميع مصادر الطاقة المتجددة، وُجِد أن الوقود الحيوي أنجعها وذلك لأنها متاحة بكثرة ولطبيعة غاز ثاني أكسيد الكربون CO_2 المحايدة. الطريقة الفعّالة والسليمة للبيئة لتحويلها إلى منتج غازي ثمين هي باستخدام طريقة حرارية-كيميائية. في هذا الصدد، الدراسة الحالية تهدُف إلى تطوير نموذج حراري-كيميائي لتحويل مادة الكتلة الحيوية لوقود غازي مفيد يسمى الغاز المتزايد Syngas. النموذج المطور بُنيَ بدمج تحويل الفحم وتشكيل القطران مع مبدأ التوازن الحراري-الحركي، ما يمكننا من حساب تركيز الغاز المتزايد. تم اختبار آثار التغير في العوامل التشغيلية – مثل: ضغط ضاغط الهواء، تكافؤ التحويل الغازيGER ، نسبة البخار إلى الكتلة الحيوية SBR، ونقطة الَقرصة لـجهاز HRSG – على أداء جهازي BIGCC و BIGCC-VAR، مثل كفاءة الطاقة والجودة الإكسرجية. وقد وُجِدَ أنهُ عند قيم منخفضة من نسبة تكافؤ التحويل الغازي أن قيمة LHV للغاز المتزايد بالإضافة إلى كفاءة الطاقة و الجودة الإكسرجية للمحول الغازي عالية لجميع مواد الكتلة الحيوية، في حين أن تأثير تكافؤ التحويل الغازي على كفاءة الطاقة والجودة الإكسرجية لجهاز BIGCC أكثر وضوحاً عند القيم العالية. كفاءة كل من الطاقة والجودة الإكسرجية للمحول الغازي تنقص بزيادة نسبة البخار إلى الكتلة الحيوية. في المقابل نجد أن كفاءة الطاقة و الجودة الإكسرجية لجهاز BIGCC تزيد بزيادة نسبة البخار إلى الكتلة الحيوية. أخيراً، نجد أن كفاءة الطاقة و الجودة الإكسرجية لجهاز BIGCC تزيد بزيادة ضغط المحول الغازي وتنقص بزيادة درجة حرارة نقطة القَرصة لجهاز HRSG. استخدام نظام التبريد الامتصاصي بسائل $LiBr-H_2O$ عند مخرج جهاز HRSG أظهر تحسناً في كل من كفاءة الطاقة و الجودة الإكسرجية لجهاز BIGCC. إدراج الخصائص الكيميائية و الفيزيائية للجودة الإكسرجية لسائل $LiBr-H_2O$ يظهر نتائج مثيرة

للاهتمام، حيث كشفت النتائج أن الحسابات التي تمت بعد أخذ هذه الخصائص في الاعتبار عن تغيير واسع النطاق على الجودة الإكسرجية للمكونات الرئيسية لدورة القدرة والتبريد المقترحة.

CHAPTER 1

INTRODUCTION

1.1 Overview

Energy plays a vital role in the development and economic growth of every nation. Due to a sheer increase of the population and living standards, energy demand is exponentially increasing which is majorly meeting out by the combustion of fossil fuels that includes oil, natural gas, coal and other carbon based fuels.

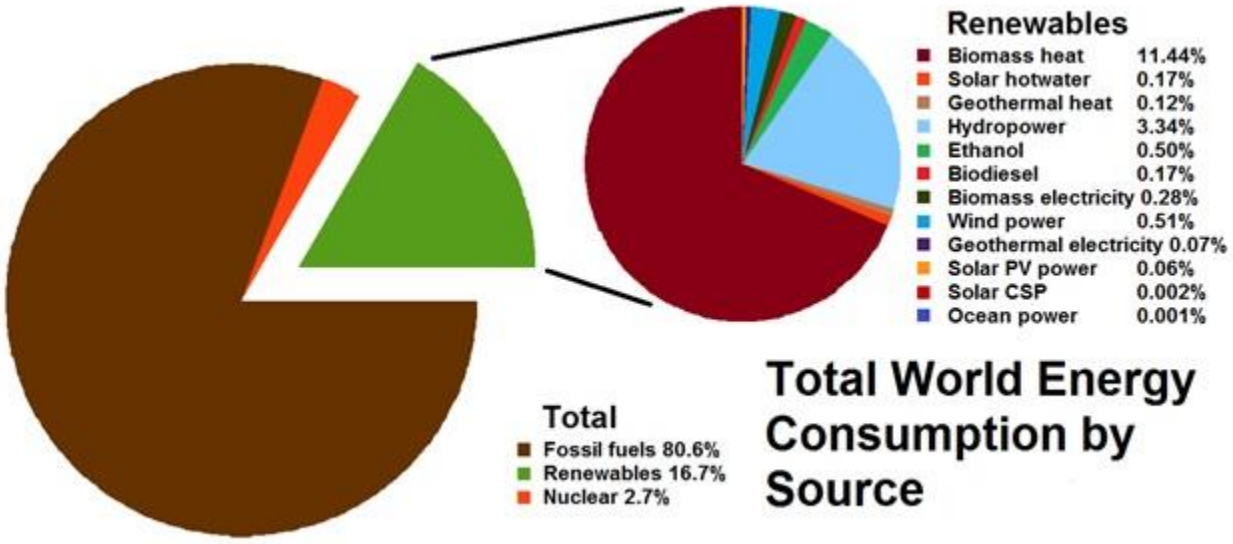

Figure 1: Total energy consumption in the world[1]

More than 80% of the total power in the world is produced using fossil fuels. Among them, crude oil (45%), natural gas (20%) and coal (15%) are the main sources of fossil fuel.

Though fossil fuels are the main source of energy it has some limitations thermodynamically and environmentally as well. The efficiency of oil fueled steam turbine power plant reaches up to 44%, for coal fired steam turbine it goes up to 47% and for gas turbine of natural gas fueled power plant is nearly 40%. The efficiency of a fossil fuel power plant can rise up to 58% in combined gas turbine power plants. There are huge losses of energy potential in burning the fossil fuels. Fossil fuels are non-renewable sources of energy and will be depleted once they are completely consumed. Their sources are inadequate and they are reducing at a faster rate as the rate of consumption of power is increasing day by day. Over consumption of fossil fuel raises environmental issues. It releases CO_2, CO, NO_x, SO_x during burning that can have severe affect in environment. Formation of CO_2 is the main reason behind global warming, CO is poisonous, NO_x and SO_x are the cause of acid rain due to the formation of sulphuric acid and nitric acid after reaction with the water vapor in the atmosphere. Global warming, ozone depletion, acid rain and photochemical smog are the main sources of environmental degradation and thus created an emergent need of utilizing the alternative sources of energy for power generation. Among all these renewable energy sources, biomass has been found as the most promising option for power generation. This is because in most of the countries biomass is abundantly available in the form of agricultural waste, solid waste, municipal waste etc. and its utilization for power generation has three-fold benefits:

- This will minimize the problems of waste disposal
- It is a CO_2 neutral fuel means to minimize the global warming
- Reduces the load on the power grid where electricity produced through fossils.

The most beneficial fact about biomass which can be said is that it is a part of the carbon cycle. There is a balance in CO_2 release from biomass and as it inhales during growing up. This energy is renewable and abundant and does not emit harmful substances.

There are traditional and unconventional methods for the conversion of biomass into fuel that may be used for power generation. Direct combustion, pyrolysis and gasification are the most commonly used methods. Direct combustion of biomass results in the formation of harmful pollutants like; CO, UHC and fuel-burned NO_x. This compelled the researchers to find clean and efficient waste to energy methods. Gasification of biomass is thermo-chemical technology that converts the biomass into the hydrogen enriched producer gas called syngas while utilizing the gasifying agents. Gasification is cost-effective at every limit of power production abilities from 5 kWe onwards. Therefore, there is endless and steady attention in the production of energy from biomass through gasification. From time to time, several explanations are reported to describe the complex phenomena of biomass conversion. A time has now come to reexamine the gasification process to bring out the role of categorization of biomass. Depending upon the nature of the environment, inert and reactive, prevailing during gasification, the process is called pyrolysis for the inert environment and gasification for the reactive environment.

1.2 Gasification

1.2.1 Main Stages of Gasification

Gasification is a thermochemical method that converts biomass into the syngas i.e. (CO, H_2, CH_4, CO_2,H_2O) at high temperature in the presence of gasifying agent namely air ,oxygen, steam or mixture of these components. The temperature in the gasifier needs to

be raised up to 600ºC to 1000ºC to gasification to occur. To rise up the temperature, heat is added to the system. In the presence of a gasifying agent at elevated temperature, the large molecules of biomass converts into lighter molecules and finally to permanent gasses, char, tar and ash. Char and tar are present if the complete conversion does not take place. The overall reaction in the proceeding of gasification follows multiple reactions in the pathway.

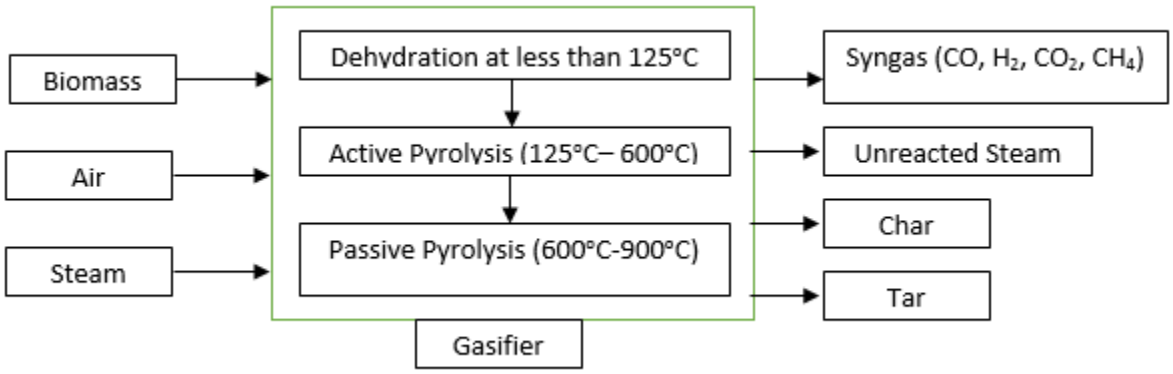

Figure 2: Main stages of gasification

1.2.2 Main Reactions Occur During Oxidation and Reduction in Gasifier

The complex process of gasification can be described as the series of oxidation and reduction reactions given below:

$$C + O_2 \leftrightarrow CO_2 , \Delta H = -393.5\ kJ/mol$$

$$C + \left(\frac{1}{2}\right) O_2 \leftrightarrow CO , \Delta H = -110.5\ kJ/mol$$

$$C + CO_2 \leftrightarrow 2CO, \Delta H = 172.4\ kJ/mol$$

$$C + H_2O \leftrightarrow H_2 , \Delta H = 131.3\ kJ/mol$$

$$C + 2H_2 \leftrightarrow CH_4 , \Delta H = -74.8\ kJ/mol$$

$$CO + H_2O \leftrightarrow H_2 + CO_2 \, , \Delta H = -41.1 \, kJ/mol$$

$$CO + 2H_2 \leftrightarrow CH_4 + H_2O \, , \Delta H = 206.1 \, kJ/mol$$

1.2.3 Types of Gasifiers

There are four categories of gasifiers based on the fact that how the fluid inside the gasifier is moving. The types are shown as the configuration below [2]

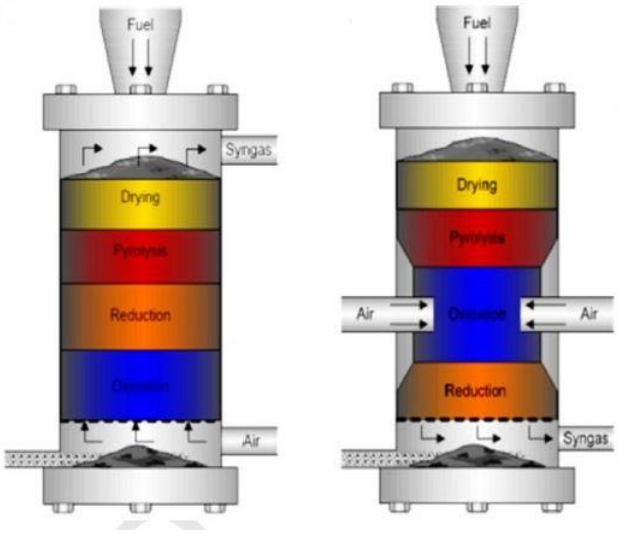

Figure 3: Updraft and downdraft gasifier

Among all the gasifiers' downdraft, updraft and circulating fluidized bed gasifier is the most common in commercial use. Selection of a gasifier depends on largely the purpose of gasification, the amount of heat need from syngas and the particle matter or the kind biomass that is going to be used. Fixed bed type gasifiers are mostly used in medium scale applications and thermal efficiency is very high for these kinds of gasifiers. Downdraft type gasifier is mostly recognized for tar content in the syngas. It takes large space and needs higher investments in generating higher energy output. Updraft type of gasifier is mostly used for heating purposes. Its exit gas temperature reaches up to 250^{o}C. It can handle large range of particle size in feedstock

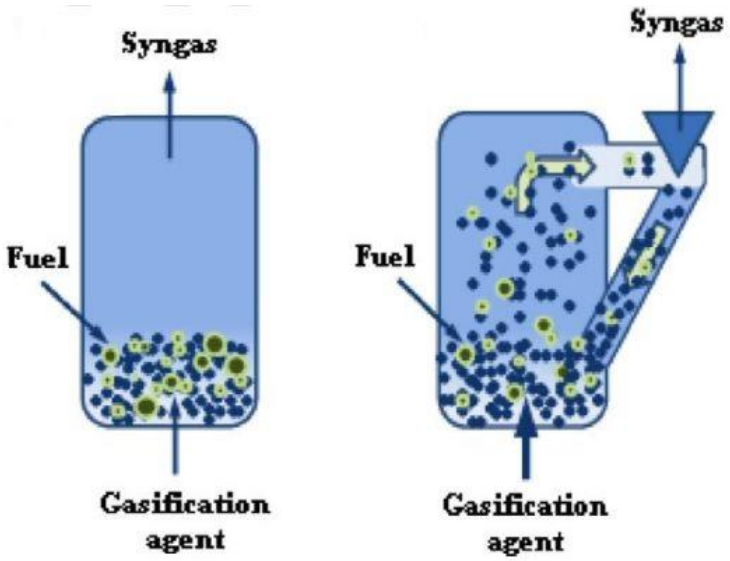

Figure 4: Bubbling bed and circulating bed gasifier

Fluidized bed type gasifier required small space compare to fixed bed type. Energy utilization for running fluidized bed gasifier is higher as external work in fan need to be provided to fluidize the biomass. Its resident time is very less compared to fixed bed gasifier and it gives higher energy output. It provides higher output than those with a fixed bed. Mass and heat transfer from the fuel can be increased considerably through fluidization and thereby increasing heating value of the output and higher gasification efficiency.

1.2.4 Gasifying Agents

There are certain agents that are used to gasify biomass. Air, oxygen and steam or mixing of these three components are used to gasify biomass to get the optimum output. Although Air gasification is commonly used due to its economic aspects, its higher heating value is lower for the presence of N_2 in the air. Gasification with oxygen or steam produces higher heating value in syngas compared to air. In industrial applications, steam injection is

commonly used in the presence of external heat resources to get optimum syngas composition.

1.2.5 Description of Various Models Utilized to Predict the Composition of Syngas

Mathematical models can be utilized to simulate an energy conversion process and analyzing its performance under varying conditions. There are mainly three kinds of mathematical models that are available to predict the syngas composition i.e. kinetic mathematical model, equilibrium model and artificial neural networks (ANN) models. Kinetic mathematical models are most complex and detailed descriptive model to predict the performance of the gasifiers. It takes into consideration the kinetic mechanisms of the biomass gasification process, various chemical reactions and transfer phenomena among phases. Equilibrium models based on chemical reaction equilibrium and take into account the overall mass and heat balances for the entire gasifier. Artificial neural networks (ANN) models co-relate the input and out data by using ANN function that has no prior knowledge of the process[3].

1.3 Integrated Gasification Combined Cycle (IGCC)

Integrated gasification combined cycle (IGCC) is considered as one of the most important power generation systems for future coal/biomass utilizations and is being promoted throughout the world as it provides power at enhanced efficiency while decreasing the emissions. An efficiency of more than 40% can be achieved through the use of biomass-fired IGCC which is the integration of Brayton and Rankine power cycles. The gasification of biomass materials necessitates marginal fuel processing and its application in combined cycle plants deliver a sustainable power generation [4][5].

Syngas produced from biomass has a very low amount of carbon content which enters the gas turbine combustor that produces clean emissions. Exhaust gas from gas turbine runs through heat recovery steam generator (HRSG) which produces high-pressured steam to run a steam turbine. Part of the steam is extracted to take as input in biomass gasifier and rest of it produces electrical power. In the combined cycle, heat losses have been taken care of using HRSG and emission has been controlled using the much pure gas. Utilization of waste heat enhances the cycle efficiency and reduces the emissions associated with the flue gasses of waste heat. The drawback of this kind of power plant is the initial cost as it is high when it is compared with pulverized coal power plants and natural gas power plants. But in the long run, if the Green House Gas (GHG) emission is taken into account then IGCC is best in hand.

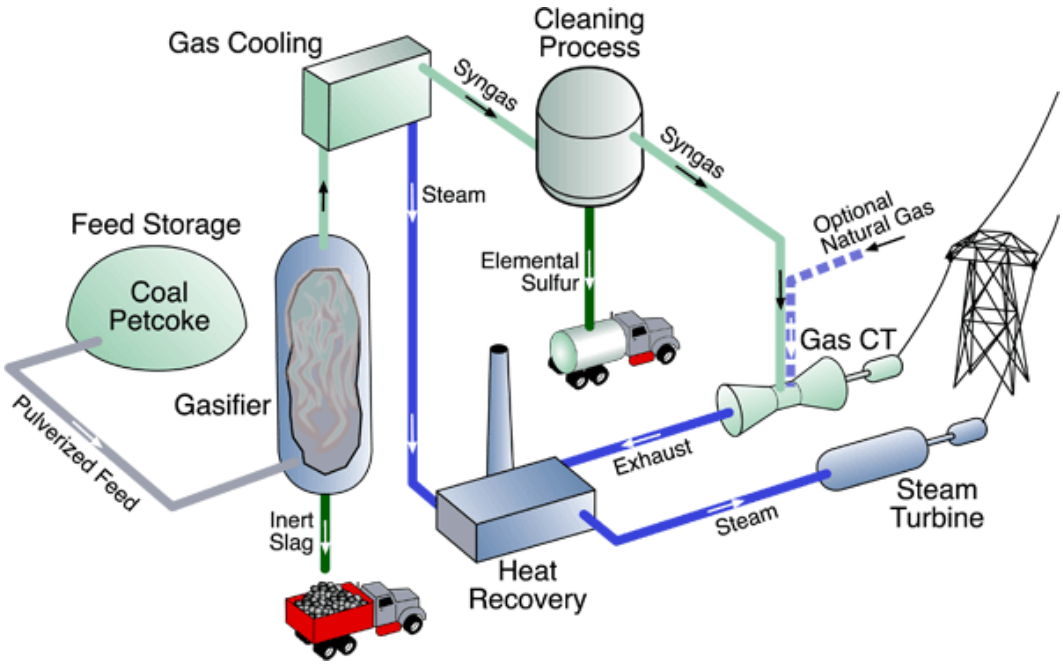

Figure 5: Schematic of a typical IGCC plant based on coal[6]

1.4 LiBr-H_2O Absorption Cooling System

Vapor absorption refrigeration systems using water-lithium bromide-water pair are extensively used in large capacity air conditioning systems. The fundamental absorption refrigeration system contains a generator, an absorber, a condenser, an evaporator, a pump, expansion valves and a solution heat exchanger (SHE). Heat is added to absorption refrigeration system generator to release the refrigerant water from the solution. In the condenser, the superheated refrigerant that comes from a generator, is condensed. Saturated liquid at condenser pressure passes through throttling valve to generate saturated liquid at reduced pressure i.e. the pressure of the evaporator. Saturated vapor after receiving heat from evaporator enters into the absorber. The mixture of LiBr and H_2O passes through solution heat exchanger and the cooled solution then passes through the throttling valve to mitigate pressure i.e. absorber pressure. Absorption temperature is kept at 35^oC at evaporator pressure. Two streams mix at absorber and form a new mixture which is pumped back through the pump and then heated in the solution heat exchanger before goes back to the generator. The cooling produces at the evaporator of the absorption system at the expense of waste heat at the exit of HRSG is the additional energy/exergy output of the cycle considered. This configuration is named as a combined power and cooling cycle operated on biomass gasifier. The recovery of waste heat results in the considerable increase of the energetic output of the cycle. Since a lesser amount of exergy is associated with the cooling output, therefore, enhancement in the exergetic output of the cycle is insignificant.

CHAPTER 2

LITERATURE REVIEW

2.1 Biomass Material

Biomass has been considered as an alternative source of energy for clean power generation and has been a key topic of research in the last few decades. Biomass covers a variety of materials such as agricultural wastes, forestry waste, and waste from paper, pulp, and sugar industry. Its utilization for power generation has the benefits of waste minimization, mitigating the global warming potential, and excess electricity to the grid. Its use for power generation has been found quite effective in CO_2 abatement [7][8]. Incineration and land filling are more commonly used techniques of biomass material handling than recycling and composting [9]. Due to its abundantly available nature, renewability, and having a neutral CO_2 potential, biomass is being widely utilized for power generation [10].

2.2 Biomass Conversion to Energy (Waste to Energy)

Waste to energy leads to the adoption of the technology that can convert biomass into the biofuels in the form of liquid or gaseous products via thermo-chemical or biochemical processes [11][12]. The most common technology for biomass conversion to higher value product is its direct combustion which is showing a tremendous potential for the utilization of biomass at large scale in the coming future [13]. Search for more effective and environmentally benign method of biomass utilization for power generation leads to the discovery of biomass gasification where the waste material is gasified in the presence of

agents and converted into the syngas which mainly consists of hydrogen and carbon monoxide. Gasification found to be potentially more efficient and clean compared to combustion, for power generation [14]. Gasification of biomass gained a wide popularity as a waste to energy conversion method and began in the 1800s. Since then various biomass gasification systems have been developed worldwide[15]. Mark and Mike[16] studied the biomass gasification process for its application in gas turbine cycle operates in combined cycle mode. Savola [17] utilized the optimization tools for simulating a cogeneration plant of 1-20 MW for combined production of power and heating. Margaret and Pamela [18] in their investigation found that very low level of NOx and PM comes out from biomass system during conversion of waste to energy. Literature is considerably classified on the methods of gasification through the use of gasifying agents. Some common routes of biomass conversion to higher value fuel were syngas from the oil processing [19], syngas from biomass derived char [20][21], and syngas from the reforming of biomass energy conversion [22]. Panigrahi et al.[19] utilized the concept of steam gasification of biomass-derived oil for syngas production. Different gasifying agents were tried like a mixture of CO_2 and N_2, H_2. The commonly used gasifying agents are; oxygen, air, air and steam together. The gasifying agent is chosen as per the requirement of the gas composition and the economics of the process. Air has been considered as the economically viable and effective gasifying agent and is commonly used for gasification in power generation [23][15][24]. It is noticed that air gasification has the demerits of producing the highly nitrogen-diluted and poor quality gas product with (8-14%) contents of hydrogen and heating value (4-7 MJ/m^3) which is not suited to second generation biofuels [25][26][27][28]. Narvaez et al. [29] studied bubbling fluidized bed air gasification of

sawdust and examined the effect of change of the gasification equivalence ratio on the energy contents of produced gas. Gasification equivalence ratio has been found as the most effective parameter as it determines the degree of reaction as well as the temperature and governs the processes of char conversion and tar formation. Utilization of pure oxygen as an agent provide a higher quality nitrogen-free gas with a LHV of 10-14 MJ/m^3 which is considerably higher than pure air gasification [26]. The use of oxygen found to be expensive as it requires the air separation unit, particularly for small scale applications up to 50 MW[30]. The air-steam biomass gasification process has been considered as the most promising option for the production of syngas from biomass material and received a considerable attention in the last couple of decades which resulted in its wide publications[31][32][33][34].

2.3 Syngas Utilization for Useful Energy Production

The syngas produced through gasification of biomass has been tremendously used for power generation. There are few commonly used power systems like; spark ignition engine, compression ignition engine, and gas turbine engine which utilizes the biomass-derived syngas as a fuel. Spark ignition engines are mostly studied for use with synthesis gas: work by Coronado et al. [35] and Shah et al. [36] are evident of this. Compression ignition engines are more complex because auto-ignition of the synthesis gas must be assured. The auto-ignition potential of syngas improves when the syngas contains more hydrogen and less nitrogen [37]. Chacartegui et al.[38] addressed the use of synthesis gas in heavy duty gas turbines; Fagbenle et al [39] studied a combustion chamber conditions and performance when using synthesis gas as fuel. Integrated gasification combined cycle has been considered broadly for power generation from biomass-derived syngas and a

considerable amount of literature is available on their performance investigations. De Kam et al. [40] used biomass IGCC technology to generate process heat and significant amounts of electricity at dry-grind ethanol facilities of co-products by utilizing the ethanol process along with other biomass sources. Wu et al [41] investigated the operating features of 1.2 MW power generation plant that run through the gasification of rice husk. Finckh and Pfost [42] investigated the power and efficiency limits and the possibilities for enhancing efficiency. The effects of gasification conditions on the performance of IGCC plants have studied well and a much is reported in this regard [43] [24][44].

2.4 Equilibrium model for a thermo-chemical gasification of biomass

The biomass gasification process [45] has been studied in two different approaches: kinetic modeling and equilibrium modeling [46]. Kinetic modeling is a complex process to model, though it is possible to predict more precise outcomes from it. An equilibrium model is simpler than the kinetic model and can provide good approximations for gasifiers like downdraft gasifiers that operate almost in equilibrium conditions. Moreover, process parameters in the gasifier can be easily studied with thermodynamic equilibrium modeling as the calculations are free from gasifier design [46]. Many investigations are reported on thermodynamic equilibrium model development for computing the composition of syngas produced through biomass gasification. Zainal et al. [47] developed an equilibrium model to predict the composition of syngas in a downdraft gasifier. They discussed the effect of moisture content and the temperature of the gasifier on the calorific value of the syngas. Prins et al. [48] studied the effect of air and steam as gasifying agents separately and compared the results using both first and second law of thermodynamics. They concluded that the air gasification prompts the production of CO and H_2 whereas steam gasification

increases the quantity of CH_4 in syngas. Li et al. [31] developed a non-stoichiometric model to predict the syngas composition and verified the results with a circulating fluidized bed gasifier. They discussed the effect of O/C ratio of biomass and temperature of gasification. Their experiment showed that the ash circulation increased the carbon conversion and steam injection made the quality of the gas better. Jarungthammachote and Dutta [49] presented a thermodynamic equilibrium model and varied with previously done experimental results. Venkata et al. [50] conducted experiments on downdraft gasifier using cash chew shell as biofuel. Their results were in good collaboration with the model they developed. Srinivas et al. [43] studied a fluidized bed gasifier where both air and steam were utilized as the gasifying agents. The interesting part of their study was they supplied the compressed air not the ambient one. They assumed the syngas free from char and tar and developed a thermo-chemical model for gasification of biomass which paved the way for computation of the equilibrium composition of syngas produced. Huang et al. [51] designed a biomass-fueled tri-generation system for building and analyzed their thermodynamic performance. Azzone et al. [52] developed a thermo-chemical model for the simulation of gasification conditions of agricultural residues. They evaluated the quality and quantity of syngas produced by gasification of a biomass material without the consideration of tar and char and also made their comparison with the data reported in the literature. Rupesh et al. [53]carried out a comprehensive investigation of a thermo-chemical model for the gasification of coconut shell as a biomass and predicted the equilibrium composition of syngas produced. Their composition considered being as more realistic than the previously reported because they incorporated the phenomena of char conversion and tar formation. Rupesh et al.[54] compared the gasification performance of

different biomass materials in terms of gas yield and heating value of syngas. They examined the effects of gasification equivalence ratio and steam to biomass ratio on the energy contents of syngas produced after feeding a given biomass material. Above studies carried out on biomass gasification show that air-steam fluidized bed gasifiers are more attractive than the other conventional gasifiers due to their better heat and mass transfer characteristics, favorable solid-gas contact, and temperature controllability. In view of the aforementioned advantages of air-steam gasification, in the current study, it was aimed to develop a thermo-chemical model for gasification of a biomass under air-steam gasification process occurs in the fluidized bed gasifier. A computer program was made in MATLAB Software to predict the approximate equilibrium composition of syngas produced after biomass gasification with the consideration of char conversion and tar formation. The developed model provided the quantity of syngas produced in terms of the number of moles the key constituents of syngas like; CO. H_2, CH_4, CO_2. N_2 also appears in the syngas but it showed inert behavior. Further, both the energy and exergy contents of the syngas were calculated as a gasifier output and subsequently the energy and exergy efficiencies of the gasifier were evaluated for various biomasses at different operating conditions.

2.5 Biomass Integrated Gasification Combined Cycle (BIGCC) for Power Generation

Integrated gasification combined cycles have been studied widely and a much is reported in the literature on their performance analysis. Mark and Mike [16] studied the IGCC with a special consideration on biomass gasifier. They observed the effect of gasifier pressure on the power output of the gas turbine. Savola [17] in their study on IGCC suggested some methods of increasing the power output of the cycle. Kim et al. [55]studied the IGCC

technology for cogeneration applications where they considered the process heat and electricity as cycle outputs. Srinivas et al. [43]investigated the performance characteristics of IGCC based on rice husk gasification under the use of steam and air at different operating conditions. They computed the power generation capacity of IGCC, plant efficiency, and gas generation per kg of biomass supplied to the gasifier. The basic limitation with their wonderful study on IGCC was the elimination of the process tar formation and char conversion during the production of syngas. Therefore, in the current study, it was targeted to propose and analyze the IGCC operates on syngas produced after gasification of the biomass supplied under air-steam gasification with the consideration of char conversion and tar formation. Along with the calculations of the gasifier's individual performance, the thermodynamic performance of IGCC was analyzed for its power generation and efficiency. In view of observing its qualitative performance, the exergy efficiency of IGCC was also evaluated along with its energy efficiency. The performance evaluated for the configuration of IGCC considered in the current study under the specified gasification conditions of biomasses is more reliable and flexible as it considered the most general and real operating conditions.

2.6 Syngas Utilization for Combined Power and Cooling production

In some of the industrial and residential sectors, the demand for cooling exists along with the requirement of electric power. In general, the cooling demand meets out with the use of vapor compression cooling cycle which requires electricity and CFC's for their operation and becomes a source of the fast depletion of fossil fuel reserves and environment degradation. A little is reported on the proposal and analysis of biomass-derived syngas fueled combined cycles utilized for simultaneous generation of electric power and cooling.

Since a significant amount of heat is wasted as flue gasses to the environment at the exit of the heat recovery steam generator (HRSG) of IGCC, therefore, the employment of waste heat driven vapor absorption refrigeration system could be a promising option to produce the cooling required. Moreover, vapor absorption refrigeration systems utilized a working fluid as a solution which is eco-friendly and available cheaply and easily. Though they provide a low value of COP compared to vapor compression systems. Khaliq and Parvez [56]carried out a study on the thermodynamic investigation of a cycle where IGCC was integrated with the waste heat drove absorption refrigeration system. Their cycle meet out the demand of electric power and cooling simultaneously in an efficient and environment-friendly manner. Their investigation was limited to the formation of syngas without char conversion and tar formation. Therefore, in the present work a biomass-derived syngas fueled combined power and cooling cycle was considered where the syngas formation with the consideration of tar and char was considered and the cycle's performance was examined thermodynamically from both energy and exergy point of views. The results obtained in the current study found to be more authentic and reliable due to the most generalized process of gasification of biomass.

As indicated above, many researchers have carried out investigations on the process of biomass gasification and the subsequent computation of syngas composition through the application of a thermo-chemical model. A research on the energy and exergy analysis of a biomass-derived syngas fueled IGCC is equally reported for various operating conditions. However, detailed and updated literature review reveals some research gaps in the related area of work which may be reported as:

1. A scope of research was found for the development of a thermo-chemical model for the air-steam fluidized gasification of biomass with the consideration of char and tar.
2. Qualitative and quantitative performance evaluation of the gasifier in terms of its both energy and exergy efficiency at variable equivalence ratio and gasifier pressure was found as another scope of research in the area.
3. Utilization of waste heat of BIGCC through the employment of absorption refrigeration system which is expected to produce cooling in an environment-friendly manner was another scope in terms of waste heat recovery.
4. Exergy analysis which identifies and quantifies the sources of losses to determine the degree of imperfection of the system performance to advanced thermodynamic cycle provided the further scope of research in the area chosen.

2.7 Overall Objective of the Thesis

The overall objective of the thesis which is fulfilled in the present research work can be summarized as:

1. A general thermochemical model for the computation of syngas composition was developed.
2. The qualitative and quantitative performance of the gasifier has been tested under different variable operating conditions. The parameters are gasification equivalence ratio (0.3-0.6), steam to biomass ratio (0.5-1.2) and compressor pressure ratio (8-16).
3. Both energetic and exergetic assessment of a BIGCC has been made for the above parameters along with pinch point in HRSG (10K-50K)

4. Combined BIGCC-VAR cycle was examined from energy and exergy point of views. Special attention was focused on chemical exergy of LiBr-H_2O in order to make a true exergetic assessment of the proposed cycle.

CHAPTER 3

SYSTEM DESCRIPTION AND METHODOLOGY

3.1 System Description

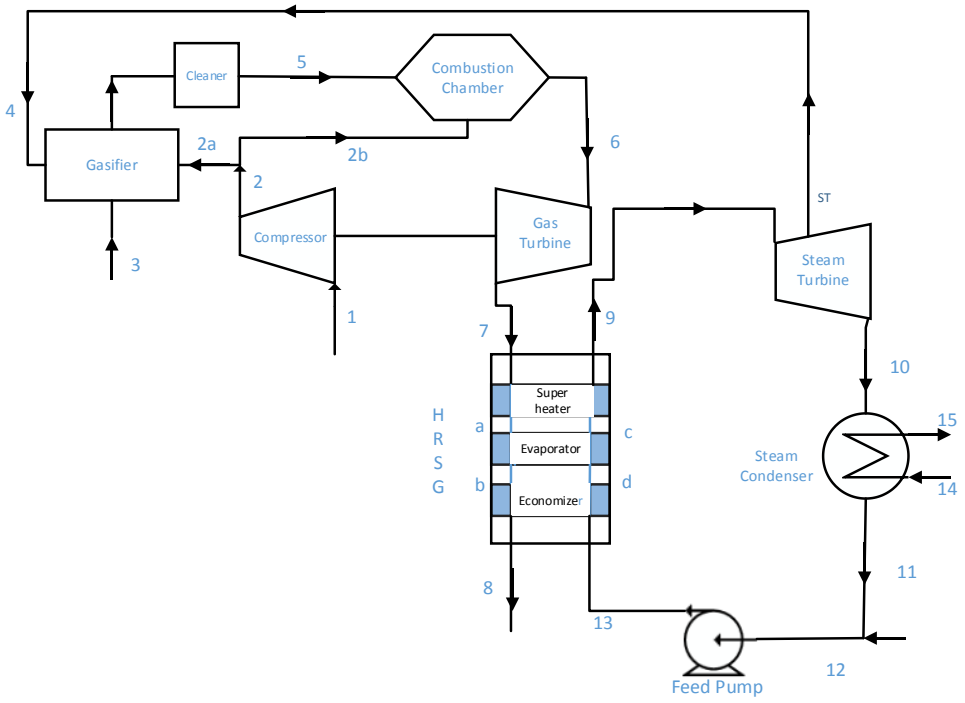

Figure 6: Schematic diagram of a biomass derived combine cycle power plant

Schematic of the proposed biomass derived combined cycle is depicted figure 6. The biomass is supplied to gasifier at ambient conditions. High-pressure air and superheated steam enter the gasifier as the gasifying agents. Biomass-derived syngas produced after gasification delivered to the combustion chamber at 5. Tar formation and char presence are shown at the gasifier exit which needs a cleaner to purify the gas

produced. The tar formation and char conversion are included in the formulation of a thermo-chemical model. Combustion products are formed at 6 after utilizing the syngas as a fuel and high-pressure air as an oxidizer. Combustion products expanded over the turbine to deliver the gas turbine power output. Turbine exhaust at higher temperature enters the HRSG and produces the superheated steam. The superheated steam at "9" delivered to the steam turbine for secondary power generation. A part of superheated steam was bled after partial expansion in the turbine at "4" and goes back to the gasifier for biomass gasification. Saturated steam leaving the steam turbine at "10" goes to the condenser where it is condensed at "11". The water is then pumped to HRSG at "13". Attention focused on combined cycle power plant clearly reveals that a considerable amount of losses in terms of energy and exergy occurs at the exit of HRSG which leads the inefficiency of the plant and environmental degradation. Therefore, in order to improve the performance of the plant from both thermodynamic and environment point of view, it is highly desirable to recover this waste heat (via flue gasses) through the use of waste heat operated energy conversion system. In this regard, a LiBr-H_2O absorption refrigeration system is employed as a bottoming cycle which is derived from the waste heat of HRSG. In the proposed cycle, a single effect LiBr-H_2O system is deployed at the exit of HRSG to produce refrigeration for space conditioning or cabin cooling. This type of cogeneration cycle can simultaneously produce both power and cooling with a single source of biomass supply and hence may result in the efficiency enhancement and emissions reduction.

The configuration of the biomass gasification combined cycle integrated with the LiBr-H_2O refrigeration system is shown in the figure given below:

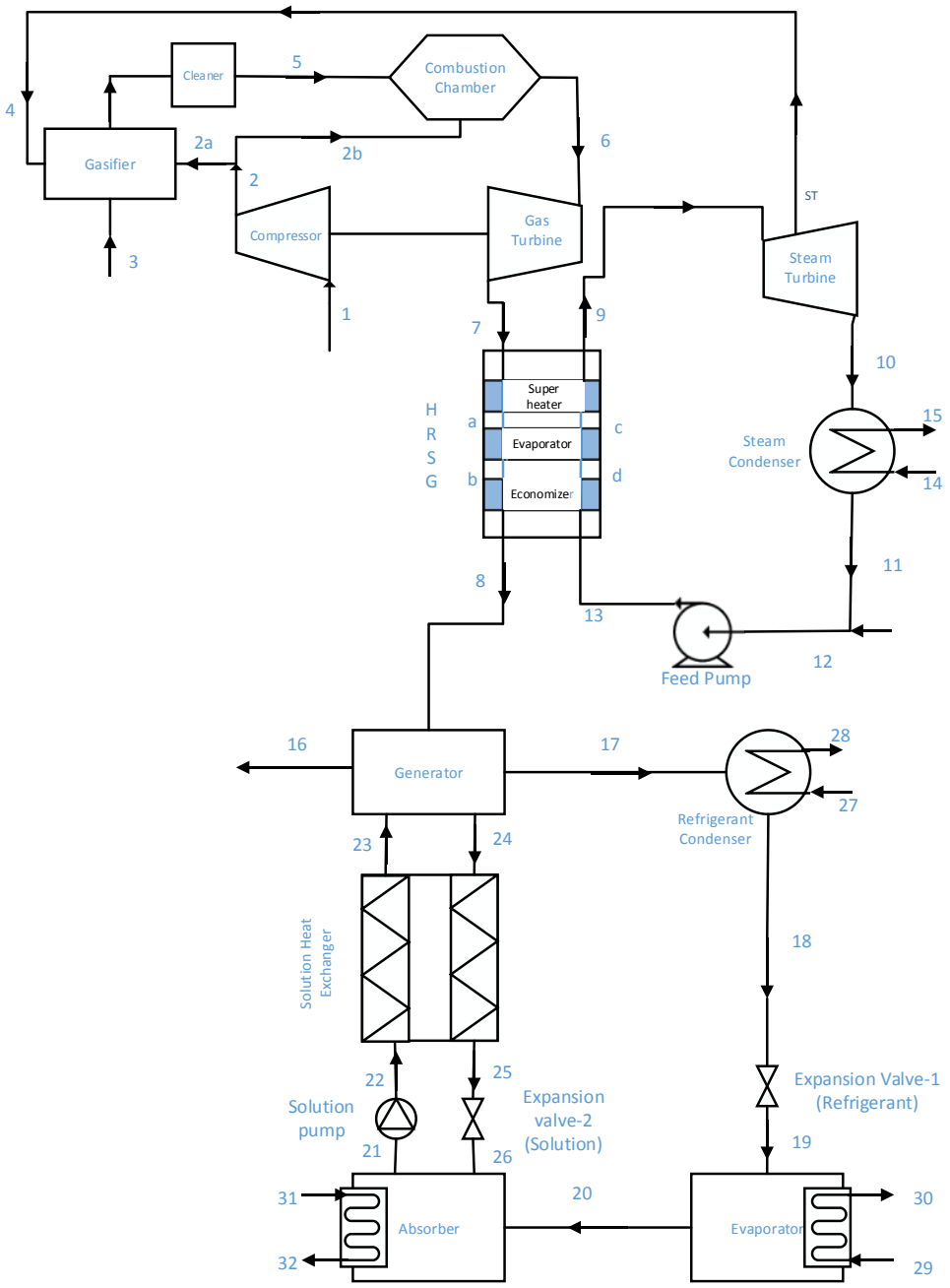

Figure 7: BIGCC with LiBr-H_2O absorption refrigeration system

3.2 Methodology

A mathematical model based on the quasi-equilibrium thermodynamic approach and some empirical relations have been developed to predict the composition of syngas produced

after air-steam gasification of biomass in fluidized bed gasifier with the consideration of char conversion and tar formation. In the model, the gasifier has been taken as a black box, which is the key component of the BIGCC where compressed air and superheated steam enters along with the biomass feed and syngas leaves as a product. The values of equivalence ratio (GER) in the gasifier, steam biomass ratio (SBR), compressor pressure ratio and pinch point in HRSG is varied to analyze the performance of the plant.

3.3 Model Formulation

A mathematical model based on equilibrium along with some empirical relations has been developed to predict the composition of syngas produced in the gasifier, incorporating the process of char conversion and tar formation. In the model, the gasifier has been taken as a black box, where the compressed air and steam flows in as the gasifying agents and the syngas flows out of the gasifier.

As biomass gasification consists of multiple complex reaction processes, making a theoretical model needs to take into account certain assumptions. The assumptions are as follows

1) C, H, O, N and Ash were taken into account in biomass ultimate dry analysis. N and Ash assumed to be inert and they do not take part in the reaction.
2) Benzene and graphite carbon are considered as Tar and Char.
3) Ideal gas formulas have been used i.e. all gasses were taken as ideal gasses
4) CH_4, CO, CO_2, H_2, N_2, H_2O, C_6H_6 (tar) and C (char) are the products coming out from the gasifier.

5) The gasification took place under the adiabatic, isobaric and steady state conditions.

6) Dried biomass was taken as input i.e. no moisture content present in the biomass which is supplied as a primary energy input to the system considered.

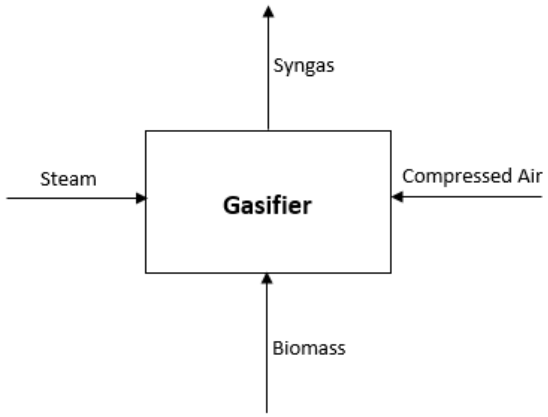

Figure 8: Basic principle of an air-steam biomass gasifier

The composition of biomasses considered in the analysis mainly consists of $C_{a1}H_{a2}O_{a3}N_{a4}$

$$\text{where } a_1 = 1 \text{ , } a_2 = \frac{H/M_H}{C/M_C} \text{ , } a_3 = \frac{O/M_o}{C/M_C} \text{ , } a_4 = \frac{N/M_N}{C/M_C}$$

A chemical formula for a selected biomass may be given as $C_{a1}H_{a2}O_{a3}N_{a4}$ where a_1 was taken as unity and a_2, a_3, a_4 were taken as the mole ratios of H, O and N with C.

The properties of biomasses tested in this study are in the following table.

Table 1: Biomass properties

Biomass	C%	H%	O%	N%	Molecular Weight (kg/kmol)	LHV (kJ/kg)	Chemical Exergy (kJ/kg)
Saw Dust	52.28	5.2	40.85	0.47	22.68	18710.69	24393.098
Coconut Shell	45.61	5.61	48.16	0.26	26.22	15969.4	22391.558

Rubber Seed	41.11	6.6	49.88	2.13	29.11	15262.81	22005.74
Corn Stalk	43.8	6.4	49.8	0	27.40	15887.01	22627.824

The global reaction for air-steam biomass gasification may be reported as follows

$$C_{a1}H_{a2}O_{a3}N_{a4} + a_5 (O_2+3.76N_2) + a_6H_2O = b_1CH_4 + b_2 CO + b_3 CO_2 + b_4H_2+ b_5H_2O+ b_6 N_2 + b_{tar}C_6H_6 + (1-\alpha)C \quad (1)$$

'a_5' and 'a_6' represents the number of moles of air and steam supplied to the gasifier, as agents of gasification, respectively. The values of 'a_5' and 'a_6' can be calculated by using the relations below for given values of gasification equivalence ratio (GER) and SFR.

$$a_5 = GER(1 + 0.25a_2 - 0.5a_3) \quad (2)$$

$$a_6 = SFR \quad (3)$$

$$SFR = \frac{M_{bio}}{M_{steam}} SBR \quad (4)$$

Molecular weight of biomass is given by

$$M_{bio} = 12a_1 + 1.008a_2 + 16a_3 + 14a_4 \quad (5)$$

Carbon conversion factor which governs the char conversion is taken as α and can be deduced after using relation below [31]

$$\alpha = 0.901 + 0.439(1 - e^{(-GER+0.0003T_g)}) \quad (6)$$

Quantity of Tar formation may be calculated after using the equations mentioned below [57]

$$Tar_{wt\%} = 35.98e^{-0.00298T_g} \quad (7)$$

$$m_{tar} = \frac{Tar_{wt\%}}{100}(1 + SBR + a_5) \quad (8)$$

$$b_{tar} = \frac{m_{tar}}{M_{tar}} \quad (9)$$

There are six unknowns in Eq. (1) but the atomic balance of C, H, O and N, gives four equations.

$$a_1 = b_1 + b_2 + b_3 + 6b_{tar} + b_c(1 - \alpha) \quad (10)$$

$$a_2 + 2a_6 = 4b_1 + 2b_4 + 2b_5 + 6b_{tar} \quad (11)$$

$$a_3 + 2a_5 + a_6 = b_2 + 2b_3 + b_5 \quad (12)$$

$$a_4 + 7.52a_5 = 2b_6 \quad (13)$$

Therefore, two more equations are required to be developed which may be formulated through two equilibrium reactions in the system and they are

Water shift reaction:

$$CO + H_2O = CO_2 + H_2$$

Hydrogasification reformation:

$$C + 2H_2 = CH_4$$

The corresponding equilibrium constant for these two equations can be written as

$$k_1 = \frac{b_3 b_4}{b_2 b_5} \quad (14)$$

$$k_2 = n_{tot}\frac{b_1}{b_4^2} \quad (15)$$

The values of k_1 and k_2 were found by using the following relations [47]

$$k_1 = exp\left(\left(\frac{5878}{T_g}\right) + \left(1.86\, log\left(T_g\right)\right) - \left(T_g\, 0.27 \times 10^{-3}\right) - \left(\frac{58200}{T_g^2}\right) - 18\right) \quad (16)$$

$$k_2 = exp\left(\left(\frac{7082.842}{T_g}\right) - \left(6.567\, log\left(T_g\right)\right) + \left(T_g 3.7335 \times 10^{-3}\right) - \left(0.3612 \times 10^{-6}\, T_g^2\right) + \left(0.0702 \times \frac{10^{-5}}{2T_g^2}\right) + 32.541\right) \quad (17)$$

In order to increase the prediction accuracy of the model, the equilibrium constants k_1 and k_2 are multiplied with c_1 and c_2 which are a function of GER of the gasifier [58]

$$c_1 = p_1\, exp(p_2 \times GER) \quad (18)$$

$$c_2 = p_3 - p_4 \times GER \quad (19)$$

p_1 to p_4 are constant numbers.

The model developed in this study for solid waste is tested by comparing the results with the published data of other researchers. Table 3 shows the comparison of the present results at the similar conditions RAFR=0.3 with the literature results. The comparison is good and agreed with previously modeled and experimented results.

Table 2: The comparison of results of gas composition related to biomass with the data from researchers

Syngas Composition (dry basis, mole %)	**Jayah et al.**[59]	**Srinivas et al.**[43]	**Altafini et al.** [60]	**Rupesh et al.**[54]	**Present Model**
CH_4	1.2	0.01	0	4.01	2.43
CO	18.9	20.3	19.7	19.4	19.47
CO_2	8.5	9.5	10.15	13.7	13.16
H_2	12.5	19.5	20.05	17.8	18.01
N_2	58.9	50.69	50.1	45.09	46.92

The above-formulated system of equations was solved by the following method

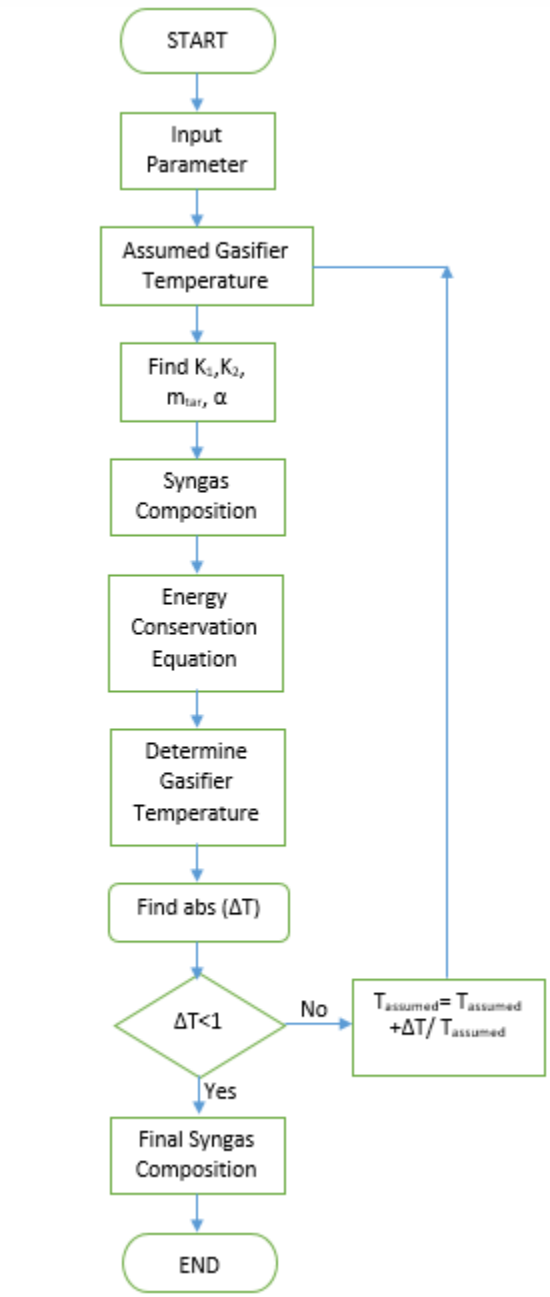

The producer gas constituents and gasification temperature are iterated using energy balance applied over the gasifier which is mentioned in Eq. (34) along with other equations mentioned above.

The lean combustion equation for the combustion chamber of the gas turbine cycle utilizing compressed air as an oxidizer can be stated as

$$\boldsymbol{b_1CH_4 + b_2CO + b_3CO_2 + b_4H_2 + b_5H_2O + b_6N_2 + a_7(O_2 + 3.76N_2) \rightarrow}$$

$$\boldsymbol{b_7CO_2 + b_8H_2O + b_9N_2 + b_{10}O_2} \quad \textbf{(20)}$$

b_7 to b_{10} and combustion temperature (T_6) are obtained using molecular balance and energy balance for the above equation [56]

3.4 Thermodynamic Analysis

3.4.1 Energy Analysis

The energy associated with working substance at a given state shown in Figure 3.1 can be defined as the following

$$\boldsymbol{H = \sum n_i(\bar{h}^o_{f_i} + \Delta\bar{h}_i)} \quad \textbf{(21)}$$

Where $\bar{h}^o_{f_i}$ the formation enthalpy and $\Delta\bar{h}_i$ is may be defined as

$$\boldsymbol{\Delta\bar{h}_i\,(T) = \int_{T_o}^{T} \bar{C}_{p_i}(T)dT} \quad \textbf{(22)}$$

$\bar{C}_{p_i}(T)$ for every element that has been taken into account are summarized in the given table [61]

Elements	Equations
CO_2	$-3.7357 + (3.0529T^{0.5}) - (0.041T) + (2.4198 \times 10^{-6}\,T^2)$
CO	$69.145 - (0.0227T^{0.75}) - (2000.77T^{-0.5}) + (5589.642T^{-0.75})$

CH_4	$-672.87 + (139.058T^{0.25}) - (0.7866T^{0.75}) + (3238.8T^{-0.5})$
H_2O	$143.05 - (58.0404T^{0.25}) + (8.2751T^{0.5}) - (0.036989T)$
N_2	$39.06 - (512790T^{-1.5}) + (10.727 \times 10^{6}T^{-2}) - (820.4 \times 10^{6}T^{-3})$
O_2	$37.432 + (2.0102 \times 10^{-5}T^{1.5}) - (178570T^{-1.5}) + (2.3688 \times 10^{6}T^{-2})$
H_2	$56.505 - (22222.59T^{-0.75}) + (116500T^{-1}) - (560700T^{-1.5})$
C_6H_6	$-0.206 + (39.064 \times 10^{-3}T) - (13.301 \times 10^{-6}\,T^{2})$
C	$1.771 + (0.771 \times 10^{-3}T) - (0.867 \times 10^{5}T^{-2})$

3.4.2 Exergy Analysis

The exergy may be defined as the maximum amount of work produced during the reversible transformation of the system from its given state to the dead state where it is in complete thermodynamic equilibrium with the environment. It can be further explained well with the figure below.

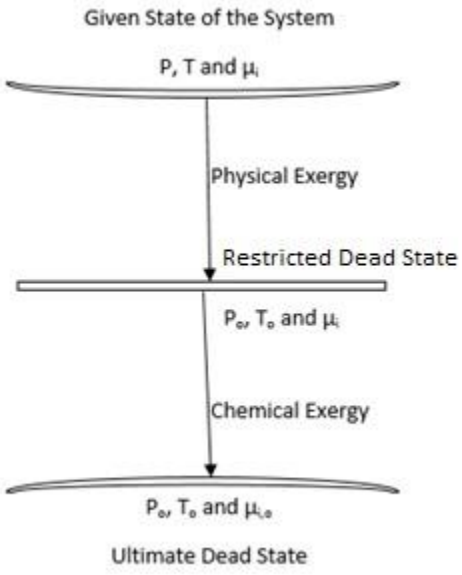

Figure 9: Exergy in stages

When the system is in a given state (figure 9), it contains physical and chemical exergy and it is due to the change of temperature, pressure and chemical compositions. When the system is in restricted dead state it in thermos-mechanically equilibrium with environment, but still it has chemical potential in it. At the ultimate dead state the system is in complete equilibrium with environment.

Mathematically, the expression for physical exergy may be stated as

$$\boldsymbol{e_{ph} = (h - h_o) - T_o(s - s_o)} \qquad \textbf{(23)}$$

Where 'e' is the specific flow exergy of the system means it is physical exergy per unit mass.

In the energy transformation processes like gasification and combustion, where the chemical composition of the working substance changes, incorporation of chemical exergy is must into the exergy analysis. This is because physical exergy deals only with the transformation of an invariable chemical composition system from given state to restricted dead state.

Thermodynamically, the chemical exergy may be defined and stated as the maximum amount of work produced during the reversible transition of a system from the restricted dead state to the ultimate dead state, and it can be expressed as

$$\boldsymbol{\bar{e}_{ch,mix} = \sum y_i \bar{e}_{ch} + \bar{R} T_o \sum y_i \ln y_i} \qquad \textbf{(24)}$$

'y_i' is the mole fraction of the 'i' component of the mixture. $\bar{R}$ is the universal gas constant in kJ/kmol–K.

Chemical exergy for at reference state for a component are taken from the table below [62]:

Table 3: Chemical exergy of different elements

Species	CH_4	CO	CO_2	H_2	H_2O(g)	O_2	N_2	C
Chemical exergy (e_{ch})(kj/kmol)	836,510	275,430	20,140	238,490	11,710	3970	690	410,802

The total exergy of the working substance per unit mass, which is a property of the substance and the surroundings, is the sum of physical and chemical exergy and is given by

$$\boldsymbol{e_{total} = e_{ph} + e_{ch}} \quad \textbf{(25)}$$

Due to the unavoidable phenomena of irreversibility, exergy destruction is associated with every component of the system which can be calculated after making an exergy balance over the component concerned. The exergetic balance applied to a fixed control volume operates under steady state is given by

$$\boldsymbol{E_D = E_{in} - E_{out}} \quad \textbf{(26)}$$

Where E_{dest} is the exergy destruction or the irreversibility of the system, E_{in} is the exergy input to the system and E_{out} is the exergy out from the system. Exergy like energy is transferred via heat, mass, and work from and to the system.

$$\boldsymbol{E_{in} = \sum m\, e_{in} + \sum Q_j \left(1 - \frac{T_o}{T_j}\right)} \quad \textbf{(27)}$$

$$\boldsymbol{E_{out} = W + \sum m\, e_{out}} \quad \textbf{(28)}$$

Where 'Q_j' is the heat transfer to the system, 'W' is the mechanical work supplied by the system, 'e' is the exergy transfer associated with the stream of matter and 'm' is the mass containing the energy. 'e' can be designated as Eq. (25)

3.5 Analysis of Individual Component of BIGCC

3.5.1 Compressor

Atmospheric air enters at 1 in the compressor at the compression pressure ratio r_c and compressor isentropic efficiency η_c

The actual temperature of air at the compressor exit can be computed after using the equation [63]

$$\boldsymbol{T_2 = T_1 + \left(\frac{T_1}{\eta_c}\right)\left(\left(r_c^{\frac{\gamma-1}{\gamma}}\right) - 1\right)} \quad \textbf{(29)}$$

Work supplied to compressor

$$\boldsymbol{W_c = H_2 - H_1} \quad \textbf{(30)}$$

Exergy destruction in compressor

$$\boldsymbol{E_{D_{com}} = E_1 + W_c - E_2} \quad \textbf{(31)}$$

Second law efficiency of compressor

$$\boldsymbol{\frac{(E_2 - E_1)}{W_c}} \quad \textbf{(32)}$$

3.5.2 Gasifier

The energy balance equation for the gasifier can be stated as

$$H_{bio} + \sum_{i=5}^{6} a_i h_i - \sum_{i=1}^{6} b_i h_i = 0 \quad (33)$$

$a_1$to a_6 and $b_1$to b_6 are described in Eq. (1)

The energy content in biomass is given by the equation [58]

$$H_{bio} = \left(\frac{a_2}{2}\right) H_{f_{H2Og}} + H_{f_{CO2}} + LHV_{bio} \quad (34)$$

The lower heating value of biomass can be determined after using the equation [64]

$$LHV_{bio} = (34.835C + 93.87H_2 - 10.8O_2 + 6.28N_2) \quad (35)$$

Where C, H, O and N are the mass percentage of the corresponding element

The lower heating value of syngas may be computed from the following equation [61]

$$LHV_{syn} = \frac{282993n_{CO} + 802303n_{CH_4} + 241827n_{H_2}}{M_{syn}} \quad (36)$$

The molecular weight of syngas was calculated using the following equation

$$M_{syn} = 28n_{CO} + 16n_{CH_4} + 2.008n_{H_2} \quad (37)$$

Exergy balance applied over the adiabatic and steady flow gasifier give rise the expression for destruction in gasifier

$$E_{D_{gasi}} = E_3 + E_{2a} + E_4 - E_5 \quad (38)$$

Second law efficiency of a gasifier can be defined after [54]

$$\frac{E_5}{E_{bio} + E_4} \quad (39)$$

The exergy of the biomass can be deduced using the following formulae [43]

$$E_{bio} = 410820a_1 + 119246a_2 + 1985a_3 + 345a_4 \quad (40)$$

3.5.3 Combustion chamber

Producer gas from fluidized bed gasifier (5) enters the combustion chamber and combusted in the presence of compressed air at 2b. Energy balance of the combustion chamber with the combustion efficiency, η_{cc} may be shown as[65]

$$H_5 + H_{2b} = H_6 + (1 - \eta_{cc})H_5 \quad (41)$$

Where H_5 comprises of the summation of enthalpy of all the element present in the producer gas and H_6 consists of the combustion products in the Eq. (20)

Exergy destruction in combustion chamber can be determined as

$$E_{D_{cc}} = E_5 + E_{2b} - E_6 \quad (42)$$

Second law efficiency of the combustion chamber

$$\frac{E_6}{E_5} \quad (43)$$

3.5.4 Gas Turbine

Exhaust gas temperature from gas turbine can be found after using the equation [66]

$$T_7 = T_6 - T_6\eta_{gt}\left(1 - \left(\frac{1}{r_{ex}}\right)^{\frac{\gamma-1}{\gamma}}\right) \quad (44)$$

Work was done by the gas turbine

$$W_{gt} = H_6 - H_7 \quad (45)$$

Exergy destruction in gas turbine

$$E_{D_{gt}} = E_6 - W_{gt} - E_7 \quad (46)$$

Second law efficiency of gas turbine

$$\frac{W_{gt}}{E_6 - E_7} \quad (47)$$

3.5.5 Heat Recovery Steam Generator

HRSG considered in the current study is comprised of economizer, evaporator and super heater. Exhaust gas from gas turbine enters the super heater and passes through evaporator and economizer and leaves at 8 as stack gas.

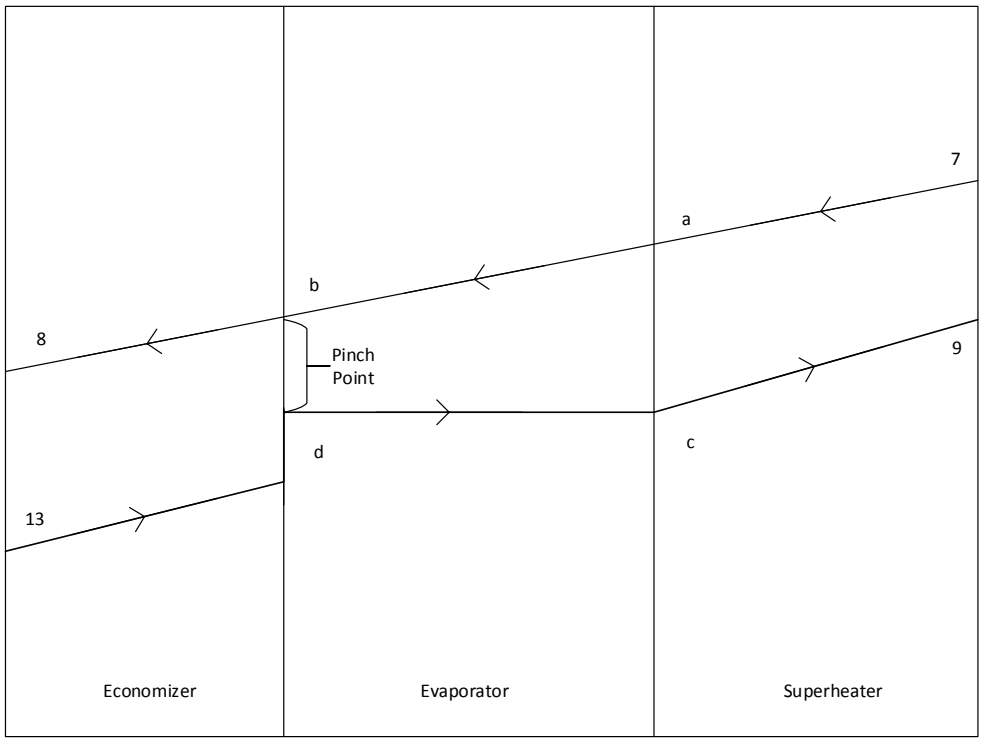

Figure 10: Pinch point temperature in HRSG

The pressurized water enters at 13 to economizer where the temperature reaches to saturation temperature at the corresponding pressure. Then it passes through the evaporator where water evaporates and temperature remains the same. The saturated steam gets

superheated from ‘c’ to 9. The waste gas temperature at point ‘b’ can be expressed in terms of pinch point and saturation temperature as

$$\boldsymbol{T_b = T_d + PP} \quad \textbf{(48)}$$

Where T_d is the saturation temperature at corresponding pressure after economizer at point‘d’. And PP is pinch point of HRSG.

The mass flow rate of steam generated in HRSG and the stack gas temperature are calculated after using the following equations

$$\boldsymbol{m_{13}(h_d - h_{13}) = H_b - H_8} \quad \textbf{(49)}$$

$$\boldsymbol{m_{13}h_{fg} = H_a - H_b} \quad \textbf{(50)}$$

$$\boldsymbol{m_{13}(h_9 - h_c) = H_7 - H_a} \quad \textbf{(51)}$$

Exergy destruction in the HRSG can be known after applying the exergy balance over the same and it gives

$$\boldsymbol{E_{D_{HRSG}} = E_7 + E_{13} - E_8 - E_9} \quad \textbf{(52)}$$

Second law efficiency of HRSG can be expressed as

$$\frac{\boldsymbol{E_9 + E_8}}{\boldsymbol{E_7 + E_{13}}} \quad \textbf{(53)}$$

3.5.6 Steam Turbine

Work done by steam turbine where a part of steam is extracted to take to gasifier as a gasifying agent can be determined after using the expression

$$\boldsymbol{W_{st} = \left(m_{13} - a_6 M_{H_2O}\right)(h_9 - h_{10})} \quad \textbf{(54)}$$

Exergy destruction in the steam turbine is known after applying

$$E_{D_{st}} = E_9 - W_{st} - E_{10} - E_4 \quad (55)$$

Second law efficiency of steam turbine

$$\frac{W_{st}}{E_9 - E_{10}} \quad (56)$$

3.5.7 Steam Condenser

The cooling media flows as stream of water at 14 carries away the heat out from the saturated vapor and results in condensation of steam at 11.

$$m_{10}(h_{10} - h_{11}) = m_{14}(h_{15} - h_{14}) \quad (57)$$

Exergy destruction in steam condenser

$$E_{D_{stm,cond}} = E_{10} + E_{14} - E_{11} - E_{15} \quad (58)$$

Second law efficiency of steam condenser

$$\frac{E_{15} + E_{11}}{E_{10} + E_{14}} \quad (59)$$

3.5.8 Feed Pump

Feed pump pressurized the water up to the selected pressure to feed to HRSG where the stream vaporizes and superheated and enters the steam turbine.

Work input to the feed pump

$$W_{fp} = m_{13}(h_{13} - h_{12}) \quad (60)$$

The enthalpy at the exit of a pump can be found using the following equation

$$h_{13} = h_{12} + \left(v_{12}(P_{13} - P_{12}) \frac{10^2}{\eta_{fp}} \right) \quad (61)$$

Exergy destruction in the feed pump is known after applying

$$E_{D_{fp}} = E_{12} + W_{fp} - E_{13} \quad (62)$$

Second law efficiency of feed pump

$$\frac{E_{12}}{W_{fp}} \quad (63)$$

3.6 Absorption Refrigeration Cycle

The exhaust gas after passing from HRSG goes through the generator (from point 8 to 16) where it boils the LiBr- H_2O solution and separate LiBr and H_2O. The strong solution of LiBr-H_2O enters the generator at point 23 and after boiling off LiBr and H_2O weak solution goes back from point 24 and released water vapor that goes from point 17. The superheated water vapor condensed and saturated liquid leaves at 18 at condenser pressure. The rejected heat of condenser is carried away by external water entering 27 and leaving at 28. The condensed water passes through an expansion valve (from 18 to 19) before going to the evaporator. The pressure and temperature go down in this process and the enthalpy remains same. The refrigerant (H_2O) reaches the saturation temperature of the evaporator pressure. The cooling effect occurs in the evaporator and that is the output of the absorption refrigeration cycle. The two-phase refrigerant passes through the evaporator (19 to 20) and takes heat from the external water (29 to 30) that becomes cool. From 19 to 20 the refrigerant water becomes vapor as the pressure of the evaporator is very low. The evaporated refrigerant then goes to the absorber and mixes with a weak solution of LiBr and H_2O that comes from point 26. This newly mixed solution is passed to solution pump

(21 to 22) to raise the pressure and through the solution heat exchanger to the generator (22 to 23). The refrigerant vapor gets energy by the cooling water (31 to 32) at the absorber that causes the incoming vapor from the evaporator to absorb heat. The solution heat exchanger performs to increase the temperature of the strong solution from 22 to 23. It takes the heat from the weak solution that leaves the generator at a high temperature and passes the solution heat exchanger from 24 to 25. The following assumptions are taken to analytically calculate the cooling effect of the system

1) The temperature in generator, condenser, evaporator and absorber were kept constant for throughout the analysis.
2) The refrigerant (H_2O) rich solution is considered as strong solution and vice versa
3) The system was taken as a steady one.
4) The pressure in each component of the system is the vapor pressure of the working fluid corresponding to the temperature of the fluid in the component.
5) Pressure drop was taken negligible in all the pipeline and components of the system
6) Expansion process in expansion valve was taken as constant enthalpy process.
7) Cooling media in condenser and absorber and heating media in evaporator was taken as water.
8) The mass flow rates of streams at various states of the system follows

$$\boldsymbol{m_{17} = m_{18} = m_{19} = m_{20} = m_r} \quad \textbf{(64)}$$

$$\boldsymbol{m_{21} = m_{22} = m_{23} = m_{ss}} \quad \textbf{(65)}$$

$$\boldsymbol{m_{24} = m_{25} = m_{26} = m_{ws}} \quad \textbf{(66)}$$

The energy balance of each component of the system results in the equations shown below

3.6.1 Generator

The heat input to the generator is the stack gas at the exit of HRSG and can be given as

$$\boldsymbol{Q_{gen} = H_8 - H_{16}} \quad \textbf{(67)}$$

Energy balance in the generator is as follows

$$\boldsymbol{Q_{gen} + m_{ss}h_{23} = m_{ws}h_{24} + m_r h_{17}} \quad \textbf{(68)}$$

Where m_{ws} and m_{ss} is the weak and strong solution mass flow rate and can be formulated as follows. [67]

$$\boldsymbol{m_{ws} = \frac{m_r x_{ss}}{x_{ws} - x_{ss}}} \quad \textbf{(69)}$$

$$\boldsymbol{m_{ss} = \frac{m_r x_{ws}}{x_{ws} - x_{ss}}} \quad \textbf{(70)}$$

In the equations before x_{ss} and x_{ws} are the mass fraction of strong and weak solution. x_{ss} and x_{ws} are the functions of T_{gen}, T_{cond}, T_{evap}, T_{abs} and can be written as [67]

$$\boldsymbol{x_{ss} = \frac{49.04 + 1.123T_{abs} - T_{evap}}{134.64 + 0.47T_{abs}}} \quad \textbf{(71)}$$

$$\boldsymbol{x_{ws} = \frac{49.04 + 1.123T_{gen} - T_{cond}}{134.64 + 0.47T_{gen}}} \quad \textbf{(72)}$$

Enthalpies of strong and weak solutions are a function of mass fraction and temperature at that point [68]. The enthalpy of vapor leaving the generator can be found using the temperature and pressure of that point [69]

Exergy destruction in the generator may be calculated after using

$$E_{D_{gen}} = E_8 + E_{23} - E_{17} - E_{16} - E_{24} \quad (73)$$

Second law efficiency of generator is given by

$$\frac{E_{16}+E_{17}+E_{24}}{E_8+E_{23}} \quad (74)$$

3.6.2 Refrigerant Condenser

The energy balance of the refrigerant condenser is as follows

$$m_r h_{17} - m_r h_{18} = m_{28} h_{28} - m_{27} h_{27} \quad (75)$$

Exergy destruction in refrigerant condenser

$$E_{D_{ref,cond}} = E_{17} + E_{24} - E_{18} - E_{28} \quad (76)$$

Second law efficiency of refrigerant condenser is given by

$$\frac{E_{28}-E_{27}}{E_{17}-E_{18}} \quad (77)$$

3.6.3 Expansion valve-1

Energy balance of expansion valve-1 leads to

$$h_{18} = h_{19} \quad (78)$$

Exergy destruction in expansion valve-1 may be calculated after using

$$E_{D_{exv-1}} = E_{18} - E_{19} \quad (79)$$

Second law efficiency of expansion valve-1

$$\frac{E_{19}}{E_{18}} \quad (80)$$

3.6.4 Evaporator

Energy balance equation in the evaporator can be given as

$$Q_{evap} = m_r(h_{20} - h_{19}) = m_{29}(h_{29} - h_{30}) \quad (81)$$

Exergy destruction in evaporator

$$E_{D_{evap}} = E_{20} + E_{30} - E_{19} - E_{29} \quad (82)$$

Second law efficiency of evaporator

$$\frac{E_{19} - E_{20}}{E_{29} - E_{30}} \quad (83)$$

3.6.5 Absorber

Energy balance equation in absorber

$$m_r h_{20} + m_{ws} h_{26} - m_{ss} h_{21} = m_{31}(h_{32} - h_{31}) \quad (84)$$

Exergy destruction in absorber

$$E_{D_{abs}} = E_{20} + E_{26} + E_{31} - E_{32} - E_{21} \quad (85)$$

Second law efficiency of absorber

$$\frac{E_{21} + E_{31} - E_{32}}{E_{20} + E_{26}} \quad (86)$$

3.6.6 Solution pump

Work input to the solution pump can be known after applying

$$\boldsymbol{W_{sp}} = \frac{\boldsymbol{m_{ss}\gamma(P_{high}-P_{low})}}{\eta_{\boldsymbol{sp}}} \quad \textbf{(87)}$$

Energy balance equation applied to solution pump gives

$$\boldsymbol{m_{ss}h_{21} + W_{sp} = m_{ss}h_{22}} \quad \textbf{(88)}$$

Exergy destruction in the solution pump can be calculated from

$$\boldsymbol{E_{D_{sp}} = E_{21} + W_{sp} - E_{22}} \quad \textbf{(89)}$$

Second law efficiency of solution pump

$$\frac{\boldsymbol{E_{22}}}{\boldsymbol{W_{sp}+E_{21}}} \quad \textbf{(90)}$$

3.6.7 Solution heat exchanger

Energy balance equation in solution heat exchanger gives

$$\boldsymbol{m_{ss}(h_{23} - h_{22}) = m_{ws}(h_{24} - h_{25})} \quad \textbf{(91)}$$

Exergy destruction in solution heat exchanger can be determined after applying

$$\boldsymbol{E_{D_{SHE}} = E_{22} + E_{24} - E_{23} - E_{25}} \quad \textbf{(92)}$$

Second law efficiency of solution heat exchanger

$$\frac{\boldsymbol{E_{23}+E_{25}}}{\boldsymbol{E_{22}+E_{24}}} \quad \textbf{(93)}$$

3.6.8 Exergy of LiBr-H_2O Solution

Though LiBr-H_2O is not an ideal solution its exergy can be calculated with the summation of physical exergy and chemical exergy. The enthalpy and entropy of the LiBr-H_2O solution have been found for a different mass fraction of LiBr in the solution. In this study the method used are the widely accepted method of Patek and Klomer [68] where the enthalpy and entropy of the solution can be found from 0 to 100 % of the mass fraction of LiBr. The chemical exergy of the LiBr-H_2O solution can be divided into two parts: standard chemical exergy and exergy destruction at the time of dissolution.

$$\boldsymbol{ex_{ch} = ex_{ch,O} + ex_{ch,dest}} \quad \textbf{(94)}$$

Standard chemical exergy of the solution can be found by the mole fraction, Molality of the solution and standard chemical exergy of each pure substance and is represented as follows

$$\boldsymbol{ex_{ch,O} = 1/M_{sol}(y_{H_2O}e_{H_2O} + y_{LiBr}e_{LiBr})} \quad \textbf{(95)}$$

Molecular weight of solution (M_{sol}), mole fractions (y_{H_2O} and y_{LiBr}) can be found with the following equations

$$\boldsymbol{y_{H_2O} = \frac{(1-x)M_{LiBr}}{(1-x)M_{LiBr}+x.M_{H_2O}}} \quad \textbf{(96)}$$

$$\boldsymbol{y_{LiBr} = 1 - y_{H_2O}} \quad \textbf{(97)}$$

Where x is the mass fraction of LiBr in the solution

$$\boldsymbol{M_{sol} = y_{H_2O}.M_{H_2O} + y_{LiBr}.M_{LiBr}} \quad \textbf{(98)}$$

$$M_{H_2O} = 18.02\ kg/kmol$$

$$M_{LiBr} = 86.85\ kg/kmol$$

Exergy destruction of the solution is the function of activity of the each pure substance and can be written as follows[70]

$$\boldsymbol{ex_{ch,dest} = \frac{\bar{R}\,T_o}{M_{sol}}\left(y_{H_2O}.\,ln\left(a_{H_2O}\right) + y_{LiBr}.\,ln\left(a_{LiBr}\right)\right)} \quad \textbf{(99)}$$

Where a_{H_2O} and a_{LiBr} is the activities of water and LiBr. The following equations are the steps to find the activities.

$$\boldsymbol{ln\left(a_{H_2O}\right) = -\phi.\nu.m.M_{H_2O}} \quad \textbf{(100)}$$

$$\boldsymbol{ln\left(a_{LiBr}\right) = -\nu.\left[ln(m) + \sum_{i=1}^{6}\frac{i+2}{i}\left(a_i + i.\frac{p.b_i}{2.\nu}\right).m^{i/2}\right]_{m}^{m_{sat}}} \quad \textbf{(101)}$$

'ν' is the dissociation number for the solute.

ϕ is the osmotic coefficient and can be found using [71]

$$\boldsymbol{\phi = 1 + \sum_{i=1}^{6} a_i m^{i/2} + \frac{p}{2\nu}\sum_{i=1}^{2} i.\,b_i\,.\,m^{i/2}} \quad \textbf{(102)}$$

a_i and b_i can be found using the following equations

$$\boldsymbol{a_i = \sum_{j=0}^{2} a_{ij}.T^{-j}} \quad \textbf{(103)}$$

$$\boldsymbol{b_i = \sum_{j=0}^{2} b_{ij}.T^{-j}} \quad \textbf{(104)}$$

a_{ij} and b_{ij} are mentioned in the table below:

Table 4: Values of a_{ij} and b_{ij}

	j=0	j=1	j=2
a_{1j}	-21.96316	4.937232×10^{3}	-6.5548406×10^{5}
a_{2j}	-3.810475×10^{3}	2.611535×10^{6}	-3.6699691×10^{8}
a_{3j}	1.228085×10^{5}	-7.718792×10^{7}	1.039856×10^{10}
a_{4j}	-1.471674×10^{6}	9.195285×10^{8}	-1.189450×10^{11}
a_{5j}	7.765821×10^{6}	-4.937567×10^{9}	6.317555×10^{11}
a_{6j}	-1.511892×10^{7}	9.839974×10^{9}	-1.27379×10^{12}
b_{0j}	-4.417865×10^{-5}	3.11490×10^{-2}	-4.36112260
b_{1j}	3.074×10^{-4}	-1.86321×10^{-1}	27.38714
b_{2j}	-4.080794×10^{-4}	2.1608×10^{-1}	-25.175971

The molality of the solution of $LiBr/H_2O$ can be calculated as

$$\boldsymbol{m = \frac{y_{LiBr}}{(1-y_{LiBr})M_{H_2O}}} \quad \textbf{(105)}$$

m_{sat} is the molality of the solution at saturated state and was taken as 0.01897 kmol/kg

3.7 Energy and Exergy Efficiency of the Combined Power and Cooling Cycle

The energetic efficiency of the gasifier can be defined as follows

$$\boldsymbol{\eta_{gasi} = \frac{LHV_{syn}}{LHV_{bio}+H_4}} \quad \textbf{(106)}$$

The energy efficiency of the combined power cycle (BIGCC) may be defined as the ratio of energetic output to the energy of fuel supplied and may be stated as

$$\boldsymbol{\eta_I = \frac{W_{gt}+W_{st}-W_C-W_{fp}}{LHV_{bio}}} \quad \textbf{(107)}$$

The first law or energy efficiency of BIGCC with cooling output can be represented as

$$\boldsymbol{\eta_I = \frac{W_{gt}+W_{st}+Q_{evap}-W_C-W_{fp}-W_{sp}}{LHV_{bio}}} \quad \textbf{(108)}$$

Second law efficiency or exergy efficiency of BIGCC is defined as the ratio of total work output to the exergy supplied via biomass.

$$\boldsymbol{\eta_{II} = \frac{W_{gt}+W_{st}-W_C-W_{fp}}{E_{bio}}} \quad \textbf{(109)}$$

Second law efficiency of BIGCC cycle combined with absorption cooling system can be represented as

$$\boldsymbol{\eta_{II} = \frac{W_{gt}+W_{st}+Q_{evap}-W_C-W_{fp}-W_{sp}}{E_{bio}}} \quad \textbf{(110)}$$

CHAPTER 4

RESULTS AND DISCUSSION

The biomass-derived syngas fueled combined power cycle (BIGCC) was analyzed for evaluating its thermodynamic performance for given operating conditions. In addition, a combined power and cooling cycle where an absorption refrigeration system is employed at the bottom of BIGCC to produce cooling along with power is also proposed and investigated. To ascertain a parametric effect of changing the operating conditions of the cycle on its thermodynamic performance, one parameter used to vary while keeping other parameters constant. The range of selected operating parameters for the chosen BIGCC are; gasification equivalence ratio (GER) 0.3- 0.6, steam to biomass ratio (SBR) 0.5-1.2, compressor pressure ratio 8-16, pinch point temperature in the HRSG (PP) 10K- 50K. Along with these parameters, biomass was also changed as a fuel. From the literature review, it was evident that these parameters effect the system most for a dried biomass.

4.1 Effect of Change in Gasification Equivalence Ratio

Since gasifier is the most important component of the cycle considered and it can be said as a heart of BIGCC, therefore, the effect of gasification conditions on the gasifier itself and BIGCC as well as on combined power and cooling cycle are examined in detail.

Figure 11 depicted, show the effect of a change in the gasification equivalence ratio on the LHV of syngas produced in the gasifier. It is found that the LHV of syngas produced decreases significantly with the increase in GER. Among the biomasses selected, a percentage decrease of 28.94% in the LHV of syngas was observed in the case of rubber seed and 27.32% in case of coconut shell, respectively. The LHV decreases with the increase in GER due to the reason that the amount of CO_2 and N_2 in the syngas increases as GER increases. Further, it is noticed that at a given equivalence ratio the maximum LHV of syngas is in the case of rubber seed and minimum in case of sawdust. This is due to the fact that different biomasses have different chemical composition.

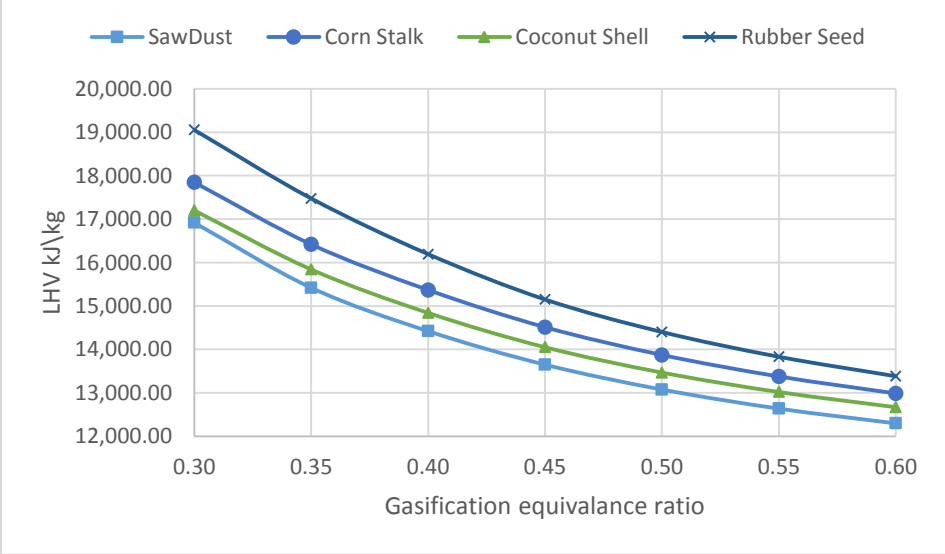

Figure 11: Effect of gasification equivalence ratio on the LHV of producer gas

The variation in the energy efficiency of gasifier with the change in GER is shown in figure 12. It is seen that the energy efficiency decreases considerably with the increase in GER. This trend is observed in parallel to the trend observed for LHV of syngas.

Since gasifier efficiency is the ratio of LHV of syngas to the LHV of biomass and energy content of H_2O, therefore any decrease in the LHV of syngas causes a corresponding decrease in the efficiency of gasifier. It is further observed that in case of saw dust as a biomass increase in GER from 0.3 to 0.6 causes a decrease in the efficiency of gasifier from 44% to 27.5%. In case of rubber seed, the gasifier efficiency decreases from 39% to 25.5% when GER increases from 0.3 to 0.6.

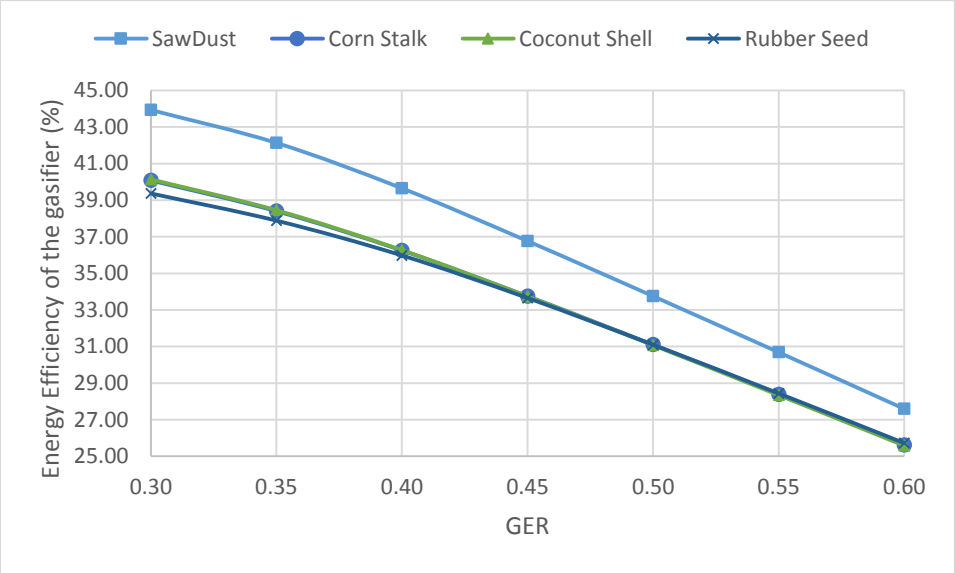

Figure 12: Effect of equivalence ratio on the energy efficiency of gasifier

Figure 13 shows the trend for variation of the exergetic efficiency of the gasifier with the change in GER. It is found that the exergetic efficiency follows the trend of energetic efficiency and it also decreases considerably with the increase in GER.

Exergetic efficiency of the gasifier depends on the exergy that is going into the gasifier and the exergy coming out of the gasifier. Biomass and superheated steam are taken as input to the gasifier. Biomass has only chemical exergy as it enters at ambient

conditions and this chemical exergy of biomass along with the physical and chemical exergy of steam takes part into the production of syngas quality which is the chemical and physical exergy of syngas. The exergy efficiency of gasifier decreases from 51% to 34% when the GER increases from 0.3 to 0.6 for sawdust. For corn stalk it decreases from 45% to 30% for the same range of GER i.e from 0.3 to 0.6. The outlet of the gasifier is syngas that also has chemical and physical exergy. Since the exergetic output of gasifier which is the sum of physical and chemical exergy of syngas is more than the LHV of syngas, therefore, the exergy efficiency of the gasifier is greater that its corresponding energy efficiency at a given GER. The production of CO, H_2 and CH_4 decreases with the increase in temperature in the gasifier.

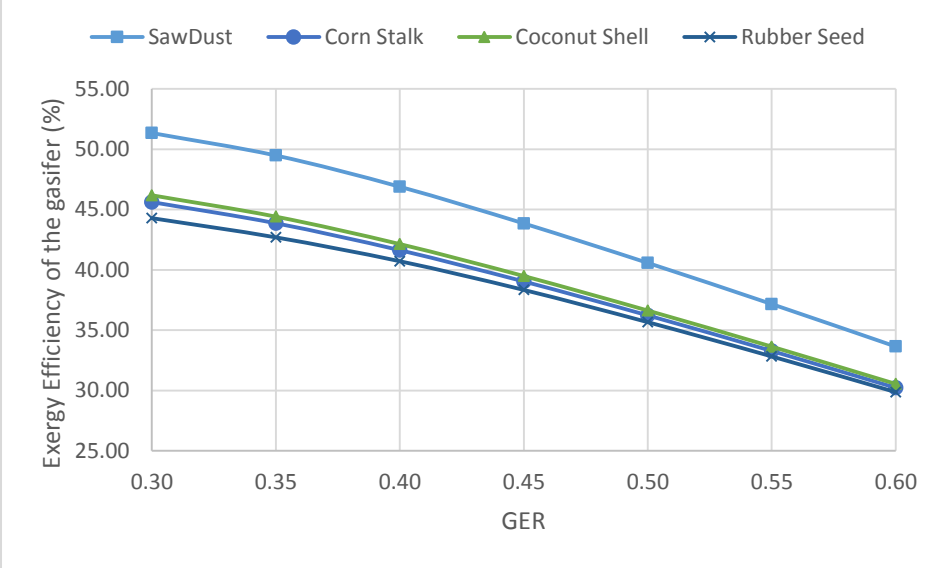

Figure 13: Effect of equivalence ratio on the exergy efficiency of gasifier

The topping cycle (BIGCC) energy output is produced from gas turbine and steam turbine and energy input to this cycle is the compressor and feed pump in HRSG. The

LHV of the biomass is converted into energy that is used in the whole cycle. The efficiency of the cycle is found using the total output energy which is a summation of the gas turbine, steam turbine work and subtraction of compressor and feed pump work. The input of the system is considered as the LHV of the biomass feedstock. Syngas produced in the gasifier is the fuel of the whole cycle. The heating value of syngas produced in the gasifier combusted in the presence of air and supplied to the gas turbine. And the exhaust gas from gas turbine passes through a HRSG to produce steam that runs a steam turbine and a fraction of that returns to the gasifier. The effect of change of GER is shown in Figure 14 where it is found that a little increase in GER initially increases the efficiency and then further increase in GER rapidly decreases the energy efficiency of the cycle. This is because during the initial rise of GER the number of moles of syngas of syngas produces increases which are a fuel to the combustion chamber. More amount of syngas produced with a little amount of air results in the increases of the mass of combustion products which in term increases the power output of gas turbine that enhances the efficiency of the combined cycle. Later on the LHV of the syngas decreases and as a result efficiency goes down as well.

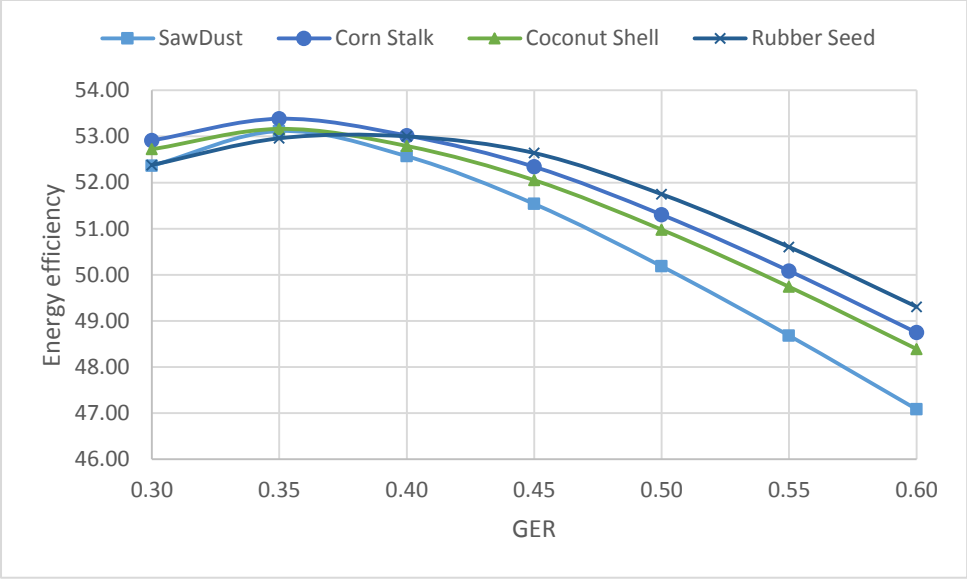

Figure 14: Effect of gasification equivalence ratio on the energy efficiency of BIGCC

In Figure 15, the effect of GER on the exergetic efficiency of topping cycle (BIGCC) is shown where it is seen that exergetic efficiency of the BIGCC increases slightly in the beginning at the increase of GER in the gasifier and then it after reaching at its peak it starts decreasing. The chemical exergy of the biomass feedstock is a primary input to the BIGCC. Since the energy content of syngas decreases as the GER increases and the syngas is a fuel supplied to the combustion chamber of BIGCC for power generation, therefore any means of reduction in the energy content of syngas causes a simultaneous decrease in power output of the cycle and hence the exergy efficiency. The reason behind the initial increase is described in the discussion of figure 14.

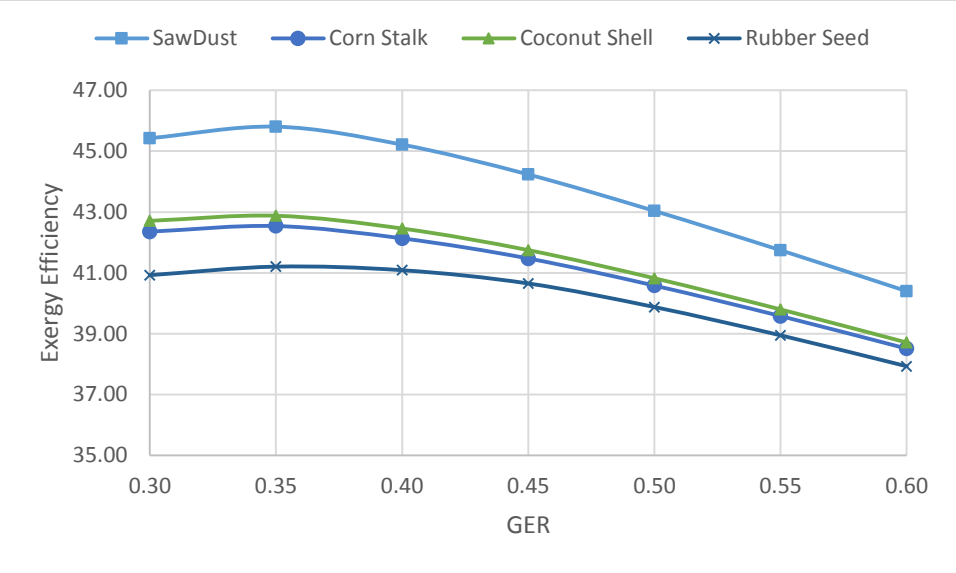

Figure 15: Effect of gasification equivalence ratio on the exergy efficiency of BIGCC

A bottoming cycle (vapor absorption refrigeration cycle) is integrated with the BIGCC which is waste heat driven and runs with the exhaust gas coming out from the HRSG of the BIGCC cycle. Simultaneous production of cooling and electric power at the expense of only biomass as a primary fuel enhances the efficiency of BIGCC. Comparison of figures 16 and 14 show that integration of VAR with the BIGCC enhances the efficiency of power generation cycle by more than a percent. The pattern of the graph follows the same as figure 14.

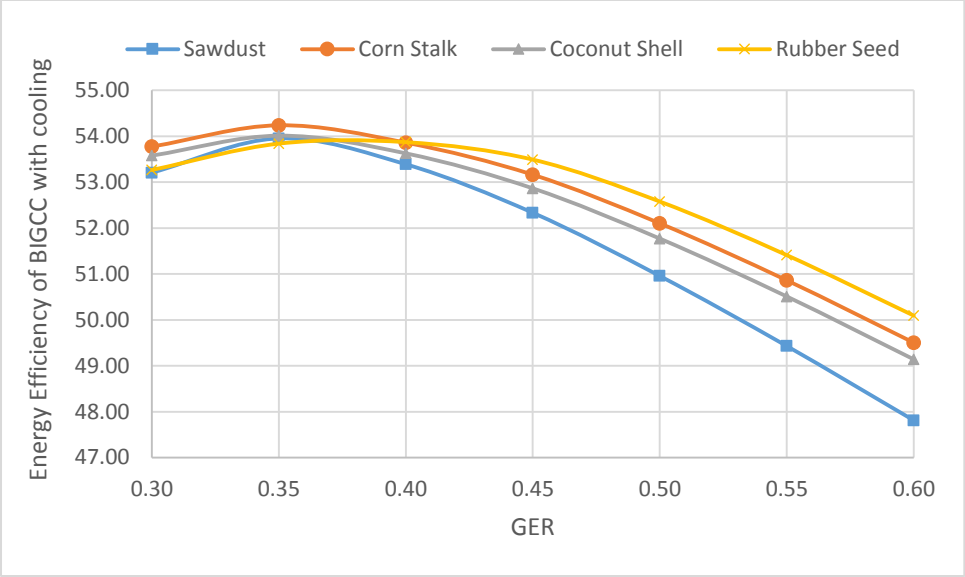

Figure 16: Effect of equivalence ratio in energy efficiency of BIGCC with LiBr-H_2O cooling system

The figure drawn on 17 represents that the exergetic efficiency of BIGCC integrated with VAR decreases with the increase of GER. Invisible increase in the exergetic efficiency of BIGCC is observed after the employment of VAR while the energetic efficiency of BIGCC increases by more than a percent. The reason for a slight gain in the exergy efficiency of BIGCC i.e. less than a percent is that amount of exergy associated with the cooling capacity of VAR is considerably less than the cooling capacity itself. Since exergetic effect of cooling appears in the numerator along with the power output in the expression of the exergetic efficiency of the combined cycle therefore this trend is observed.

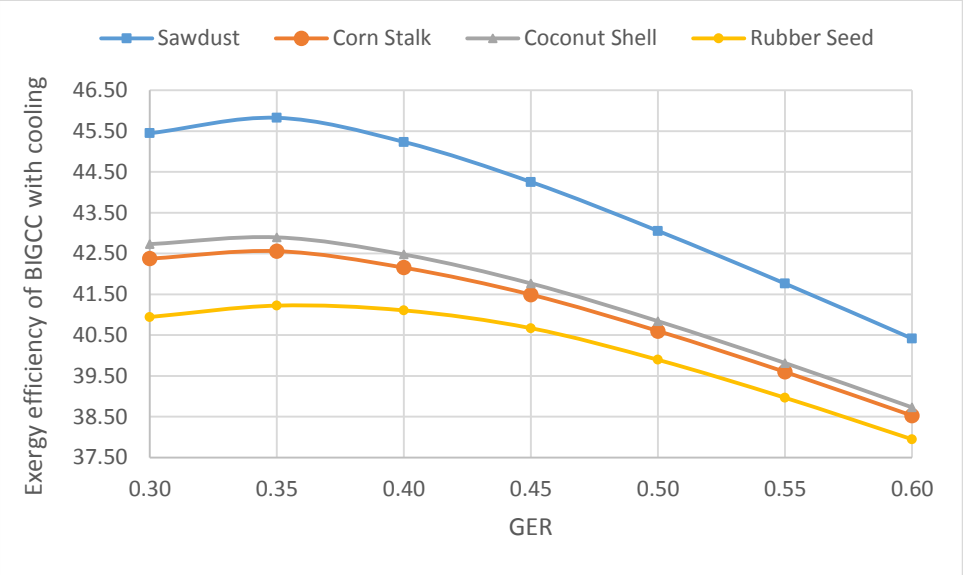

Figure 17: Effect of equivalence ratio in Exergy Efficiency of BIGCC with LiBr-H_2O cooling system

4.2 Effect of Change in Steam to Biomass Ratio (SBR)

Figure 18 show the variation of the LHV of syngas with the increase of steam-biomass ratio (SBR). It is observed that increase in SBR increases the LHV of syngas. This is because injection of superheated steam as a gasifying agent along with the compressed air results in the increase of H_2 and CH_4 content of the syngas whose LHV's are considerably higher than other species of syngas like; CO, CO_2 and N_2. With the increase of SBR the concentration of H_2 and CH_4 increases in syngas. More amount of steam and less amount of heat facilitates partial oxidation in the gasifier. It is observed that a rise in SBR from 0.5 to 1.2 causes an increase of 11% in the LHV of syngas produced after gasification of Rubber seed and 14.5% is observed in case of Sawdust gasification.

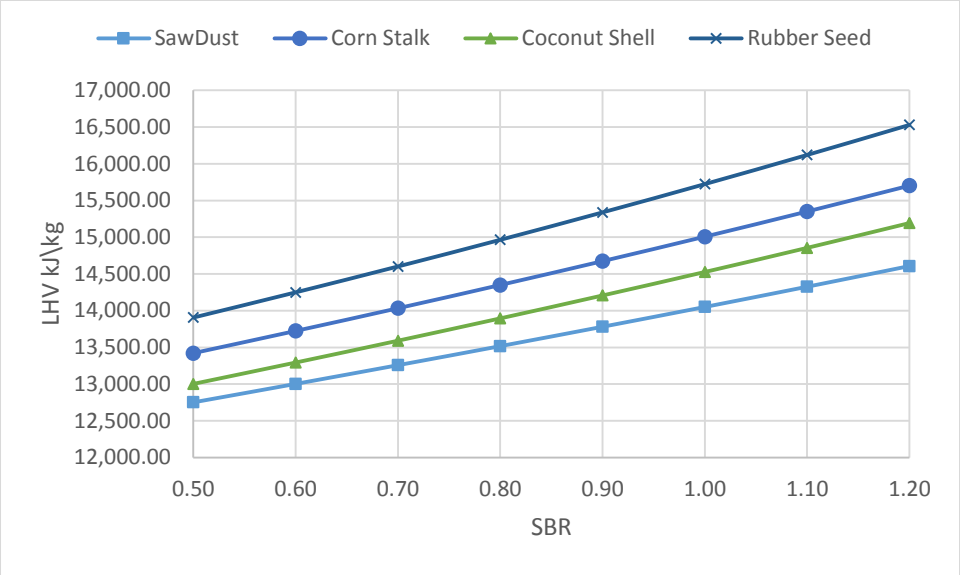

Figure 18: Effect of SBR on the LHV of the producer gas

The variation in the energy efficiency of gasifier with the change of SBR was also examined and shown in figure 19. It is seen that a rise in the SBR from 0.5 to 1.2 shows a decrease of the energy efficiency of gasifier from 43% to 32%. Since the energy efficiency of the gasifier is the ratio of the LHV of syngas and the sum of the LHV of biomass and steam therefore, any increase in the amount of steam results in the decrease of the energy efficiency of the gasifier. The energy efficiency is a measure of the overall thermodynamic performance of the gasifier assessed on the basis of the first law of thermodynamics.

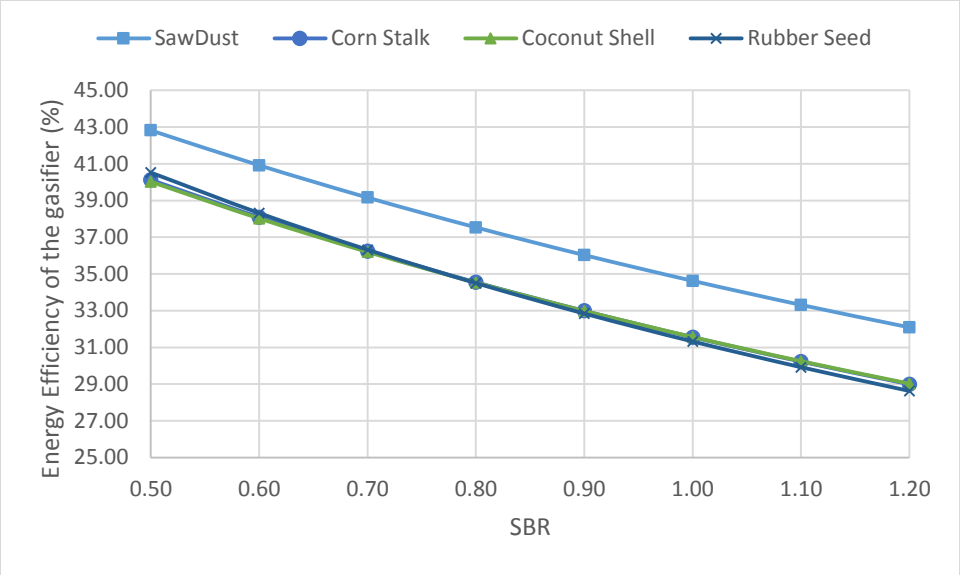

Figure 19: Effect of steam to biomass ratio on the energy efficiency of gasifier

The effect of change in SBR was also seen on the exergy efficiency of gasifier and it is shown that the exergy efficiency like energy efficiency of the gasifier also decreases with the increase of SBR. Though the decrease in the exergy efficiency is not so steep as the decrease in energy efficiency. It is seen that increase in SBR from 0.5 to 1.2 causes a decrease in the exergy efficiency of gasifier from 44.8% to 42.75. A considerable deviation is observed in the exergy efficiency of the gasifier when the type of biomass is changed. If the biomass supply is changed from saw dust to rubber seed then the exergy efficiency changes from 44.8% to 39.5%. The exergy efficiency coconut shell and corn stalk are closer to rubber seed.

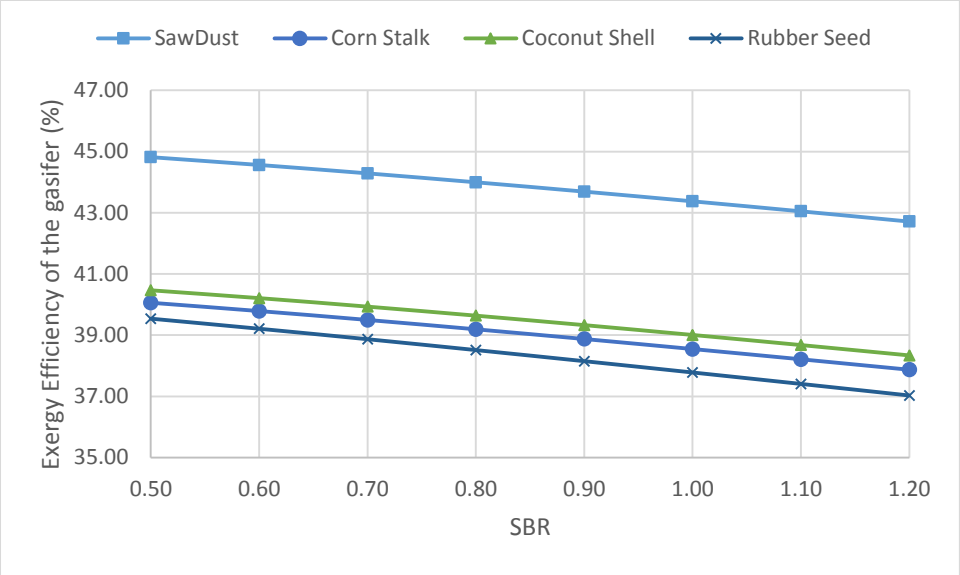

Figure 20: Effect of steam to biomass ratio on the exergy efficiency of gasifier

The effect of change in steam to biomass ratio was also examined on the energy efficiency of BIGCC which show that an increase in the SBR causes a considerable increase in the efficiency of BIGCC. It is noticed that the energy efficiency of coconut shell fueled BIGCC increases from 50.90% to 52.52%. A considerable variation in the efficiency of BIGCC is observed with the change of biomass supplied to the gasifier. As the change in biomass from coconut shell to rubber seed increases the energy efficiency of BIGCC from 50.58% to 51.59%. The variation in energy efficiency of BIGCC for different biomasses is more pronounced at lower values of SBR. By increasing the SBR the LHV of the syngas increases and thus the power output increases as well. The steam is extracted from the steam turbine at high pressure. So with the increase of injection of steam in the gasifier reduces the power output of the steam turbine but at the same time gas turbine power output increases. Overall with the

increase of steam to biomass ratio the power output of BIGCC increases which in turn increased its efficiency.

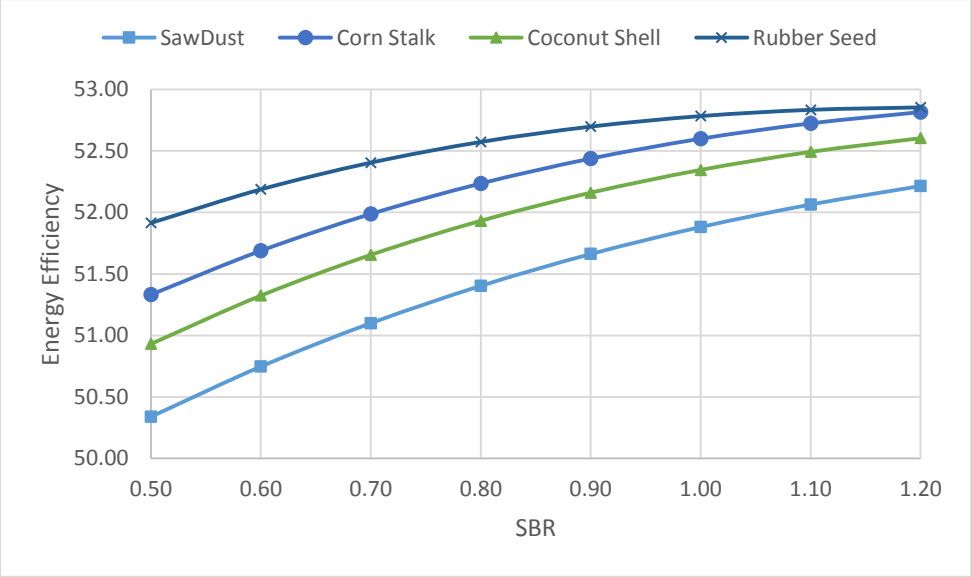

Figure 21: Effect of steam to biomass ratio on the energy efficiency of BIGCC

The effect of a change in steam to biomass ratio on the exergy efficiency of BIGCC is observed in Figure 22. It is found that exergy efficiency of BIGCC like energy efficiency increases with the increase of SBR. The exergy efficiency of BIGCC for coconut shell biomass increases from 40.4% to 42.7% when the SBR increases from 0.5 to 1.2. Change in type of biomass material also causes an appreciable variation in the exergy efficiency of BIGCC at a given SBR. Almost a constant change is observed in the exergy efficiency of BIGCC with the change in biomass material at all SBR values from 0.5 to 1.2. The exergy efficiency of BIGCC for saw dust increases from 42.9% to 45.2% when the SBR changed from 0.5 to 1.2.

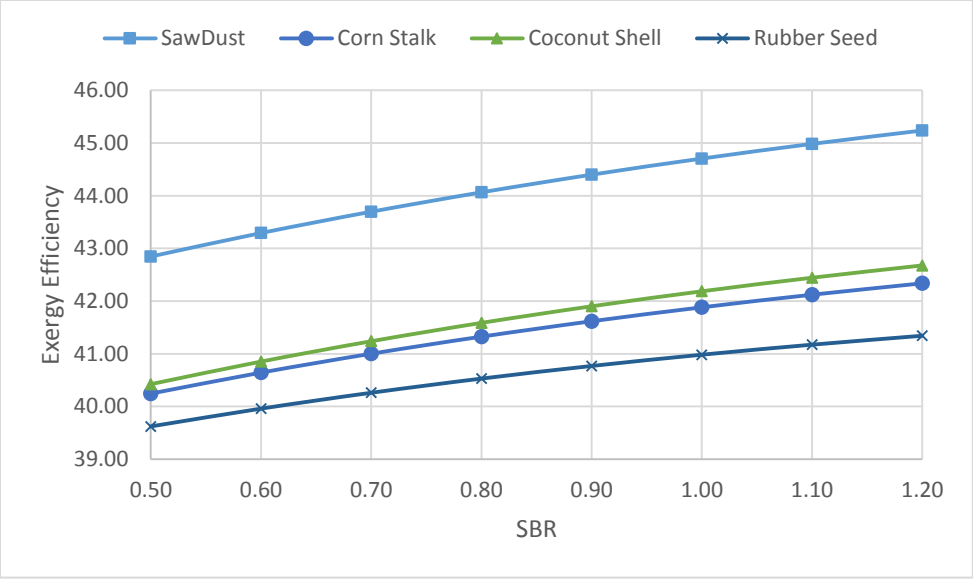

Figure 22: Effect of steam to biomass ratio on the exergy efficiency of BIGCC

Effect of employing the VAR system at the bottom of BIGCC for its efficiency enhancement is shown in Figure 23. The efficiency of combined BIGCC-VAR cycle varies considerably with the change in SBR. It is found that for dust fueled configuration the efficiency rises from 51.5% to 54.2% when the SBR changes from 0.5 to 1.2 while in the case of coconut shell the efficiency rises from 52.2% to 54.7% for the same increase of SBR. Change in biomass material causes a considerable change in the efficiency of combined BIGCC-VAR cycle. Though the trend of increase in efficiency of combined cycle appears the same as for BIGCC but enhancement in the efficiency of BIGCC after the integration of VAR is not significant which is due to the fact that the amount of cooling capacity of VAR is quite insignificant compared to the power output of BIGCC. Among all the output components the gas turbine output dominates over the steam turbine and evaporator of VAR.

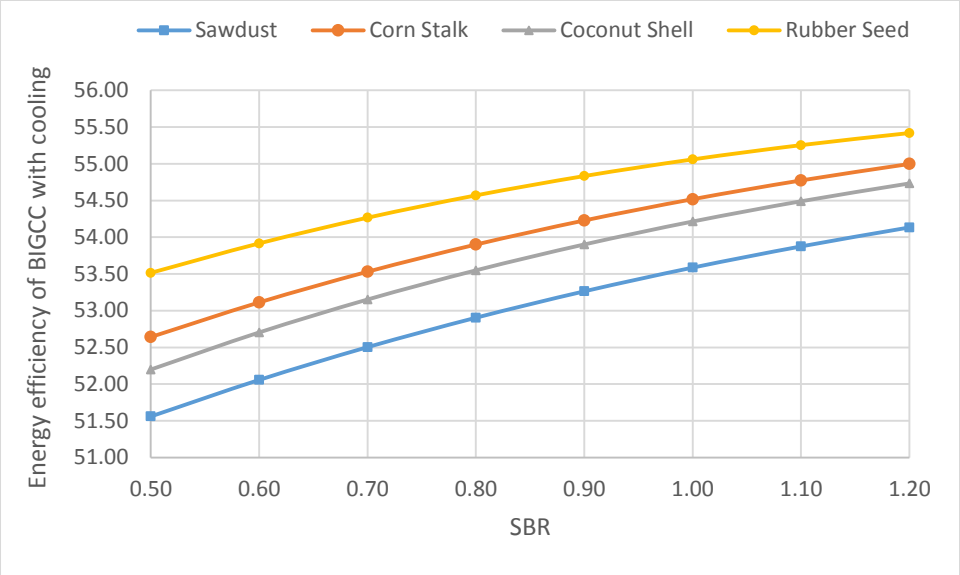

Figure 23: Effect of steam to biomass ratio in energy efficiency of BIGCC with LiBr-H_2O cooling system

The variation of exergy efficiency of combined BIGCC-VAR cycle with the change of SBR is also investigated and shown in Figure 24. It is observed that for rubber seed fueled cycle the efficiency of combined cycle increases from 39.8% to 41.5% when the SBR increases from 0.5 to 1.2. Change in biomass from rubber seed to sawdust causes an increase of the combined cycle exergy efficiency from 39.8% to 43% at the SBR of 0.5. The change in biomass material for the exergy efficiency of combined cycle is more pronounced at higher SBR. The exergy efficiency of combined cycle is significantly less compared to its energy efficiency for the given operating conditions and biomass. The rubber seed fueled combined cycle at the SBR of 0.5 attained the exergy efficiency of 39.8% only compared to its energy efficiency of 53.5%. This is due to the reason that the amount of exergy associated with the cooling produced at the evaporator of VAR is considerably less than its cooling capacity.

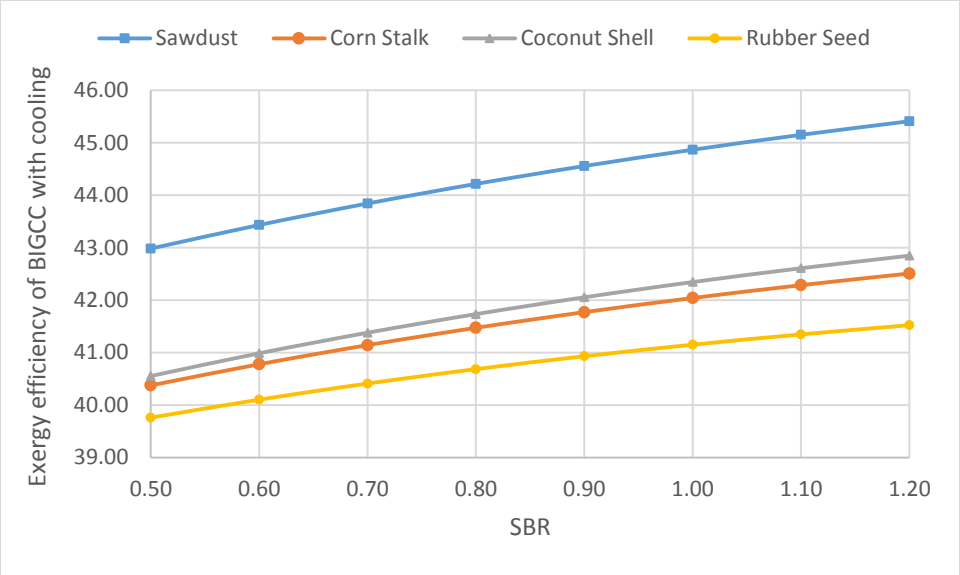

Figure 24: Effect of steam to biomass ratio in exergy efficiency of BIGCC with LiBr-H_2O cooling system

4.3 Effect of Change in Compressor Pressure Ratio

The effect of a change in the gasifier pressure on the LHV of syngas is shown in Figure 25. It is seen that the LHV of syngas decreases when the compressor pressure ratio increases. For the corn stalk gasification, the LHV of syngas reduces from 14600 kJ/kg to 14400 kJ/kg when the pressure ratio changes from 8 to 16. The effect of a change in biomass material on the LHV of syngas is almost equally pronounced at all values of compressor pressure ratio (8-16). The increase in compressor pressure ratio results in the increase of gasifier temperature which causes a decrease in the concentration of hydrogen and methane in syngas and hence its LHV. Overall a small reduction in the values of the LHV of syngas is observed when the compressor pressure ratio increased and this trend is almost same for all the selected biomasses of the study.

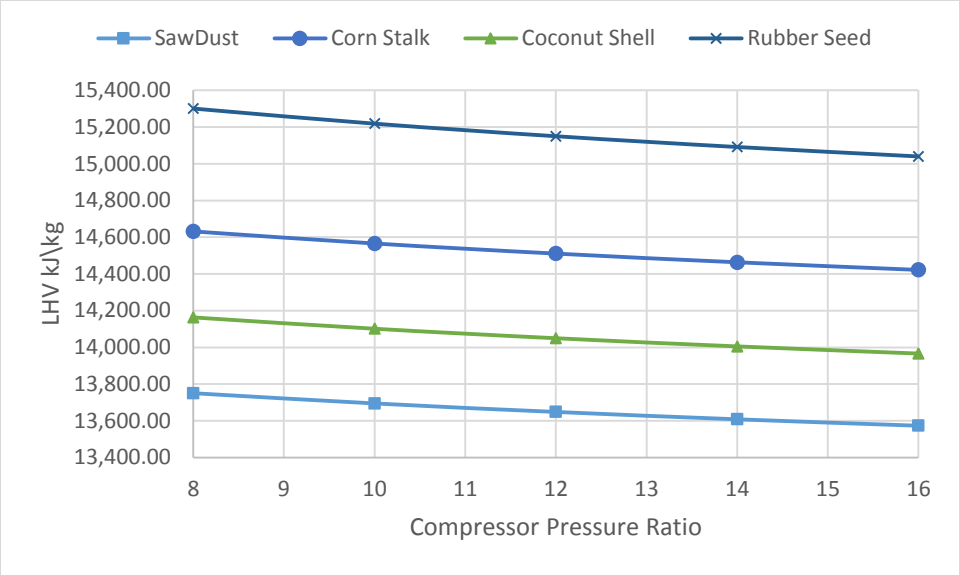

Figure 25: Effect of compressor ratio on the LHV of producer gas

The effect of change of compressor ratio on the energy efficiency of gasifier is shown in Figure 26. A small variation in the energy efficiency of gasifier is found for a large change of compressor ratio. For saw dust gasification the energy efficiency of the gasifier changes from 37% to 36.7% when the compressor pressure ratio changes from 8 to 16. Change in biomass material has a significant effect on the gasifier efficiency and it is seen that the energy efficiency of gasifier changes from 33.7% to 37% at gasifier pressure of 8 bar when the biomass changes from rubber seed to sawdust. Corn stalk, rubber seed, and coconut shell almost show the trend and values of the efficiency of gasifier at all values of the compressor pressure ratio. This is due to their similarity in the composition of syngas produced by gasification of these biomasses.

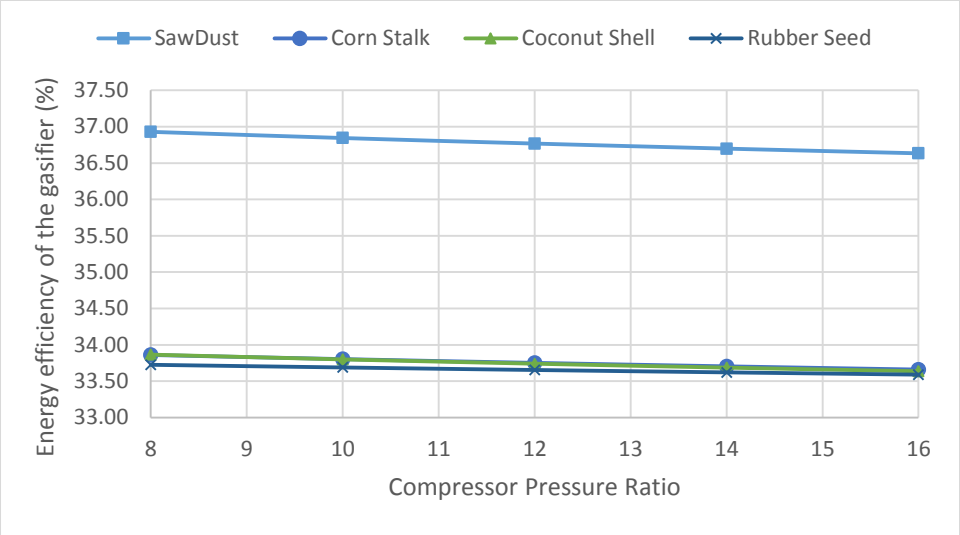

Figure 26: Effect of compressor pressure ratio on the energy efficiency of gasifier

The variation of exergy efficiency of the gasifier with the change in gasifier pressure is also examined and shown in Figure 27. It is found that change in gasifier pressure has a very little effect on its exergy efficiency as in case of saw dust gasification it is observed that the exergy efficiency decreases from 44% to 43.8% when the compressor pressure ratio changes from 8 to 16. In contrary to the energy efficiency of gasifier a visible change in the exergy efficiency of the gasifier is observed for corn stalk, rubber seed and coconut shell almost at all gasifier pressures. The exergy efficiency of saw dust gasification is considerably higher than other three biomasses. The production of the elements that constitutes the syngas decreases with the increase of gasifier pressure which results in lower exergy of syngas at the outlet of gasifier and hence the exergy efficiency.

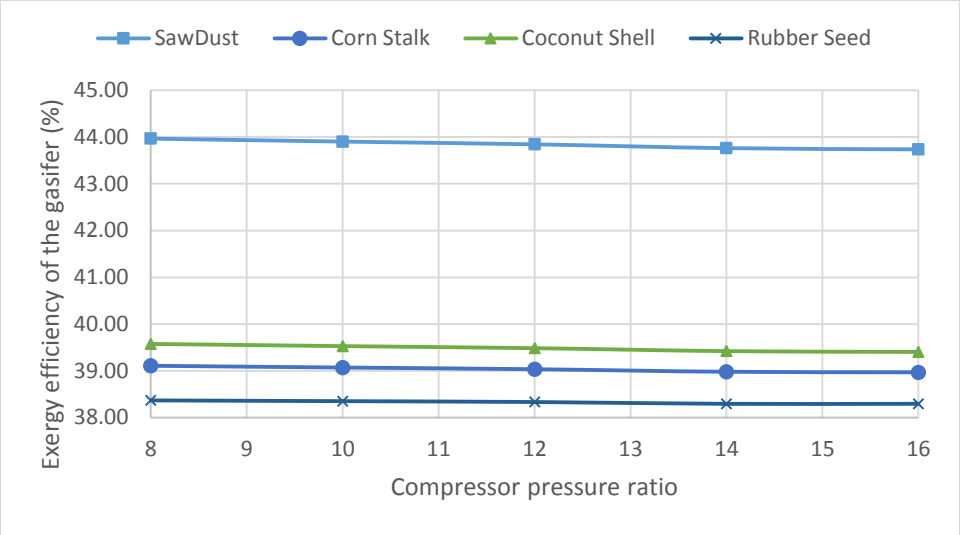

Figure 27: Effect of compressor pressure ratio on the exergy efficiency of gasifier

The energy efficiency of BIGCC increases with the increase of compressor pressure ratio as shown in Figure 28. It is seen that the energy efficiency of BIGCC increases from 50% to 52.8% when the compressor pressure ratio increased from 8 to 16 in the case of sawdust fueled BIGCC. Almost a same kind of trend is observed for all selected biomasses and the effect of a change in biomass on the energy efficiency of BIGCC is equally pronounced at all pressure ratios. The reason for increase in the energy efficiency of BIGCC with the increase of compressor pressure ratio can be stated as higher compressor pressure ratio increases means the higher gasification temperature which results in the increase of the energy contents of the streams of air and syngas which are input to the combustion chamber and the energy applied to combustion chamber reveals that the energy content of the combustion products would increase which is an inlet to gas turbine and hence its power output increased. The efficiency is increasing throughout but in the beginning, the effect of compressor pressure ratio is more pronounced and it is found that when the pressure ratio changes from 8 to 12 the

efficiency changes linearly and beyond 12 the increase in efficiency slow down and continue till 14 and increases afterward linearly. This is because the increase in compressor pressure ratio increases the energy consumed by the system and from 12 to 14 it is found more dominant that effects the efficiency. Since the LHV of syngas decreases with the increase of compressor pressure ratio which means a further increase of compressor pressure ratio more amount of syngas may be required in the combustion for a given power output.

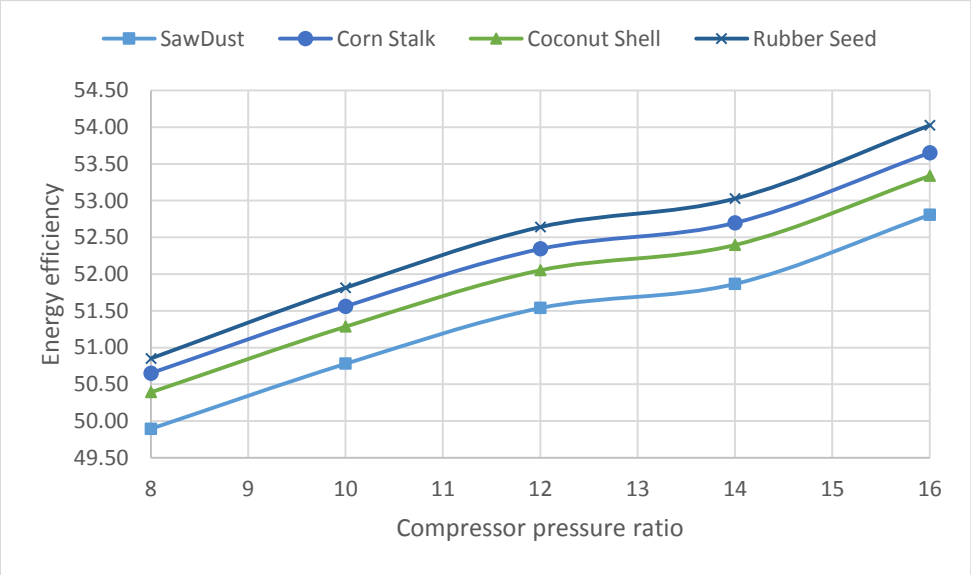

Figure 28: Effect of compressor pressure ratio on the energy efficiency of BIGCC

The exergy efficiency of the BIGCC is also investigated with the change of compressor pressure ratio and is shown in Figure 29. It is observed that the exergy efficiency of BIGCC increases with the increase of pressure ratio but a little rise in the exergy efficiency appears for a large change of pressure ratio. The change in biomass has a considerable effect on the exergy efficiency of BIGCC and is almost equally pronounced at all selected values of gasifier pressure. The reason for the increase in the exergy efficiency of BIGCC is similar

to that explained in the discussion of Figure 28. The exergy contents of syngas are more that its energy contents but due to the highly irreversible nature of combustion chamber the exergy of combustion products is less than their energy contents due to which increase in exergy efficiency of BIGCC are comparatively less than its energy efficiency.

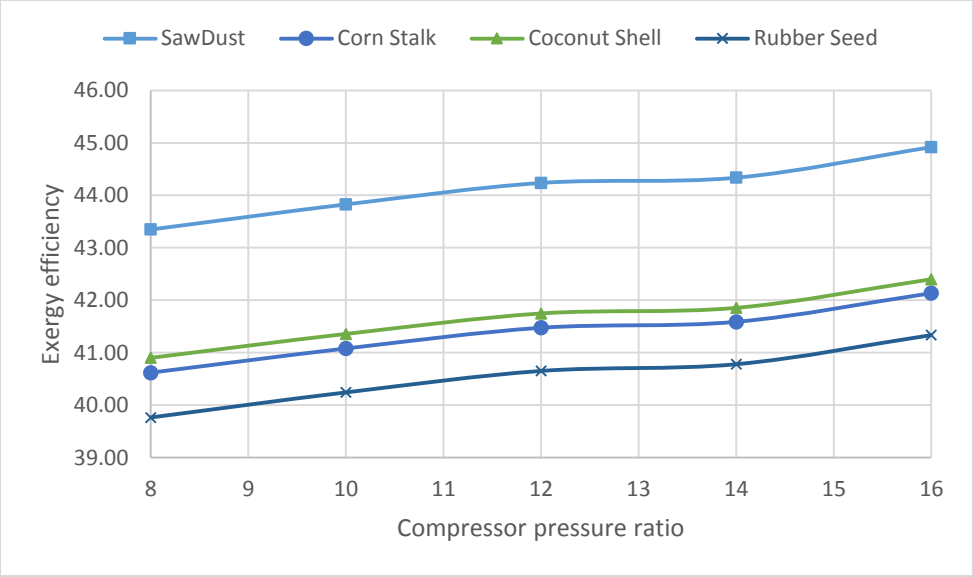

Figure 29: Effect of compressor pressure ratio on the exergy efficiency of BIGCC

The effect of a change in compressor pressure ratio was also investigated on the energy efficiency of BIGCC combined with the VAR and is shown in Figure 30 where it is seen that combined cycle's energy efficiency increases with the increase of pressure ratio. For the coconut shell fueled combined cycle the energy efficiency rises from 51.2% to 54.1% when the compressor pressure ratio increased from 8 to 16. The effect of a change in biomass on the energy efficiency of combined cycle also appears and the deviation in efficiency is almost same at all selected values of gasifier pressure. Comparison of Figure 28 and 30 show a slight increase in the efficiency of BIGCC with the employment of VAR system. This is due to the fact the cooling output of VAR

is significantly less than the power output of BIGCC. The trend of the figure is described in the discussion of figure 28.

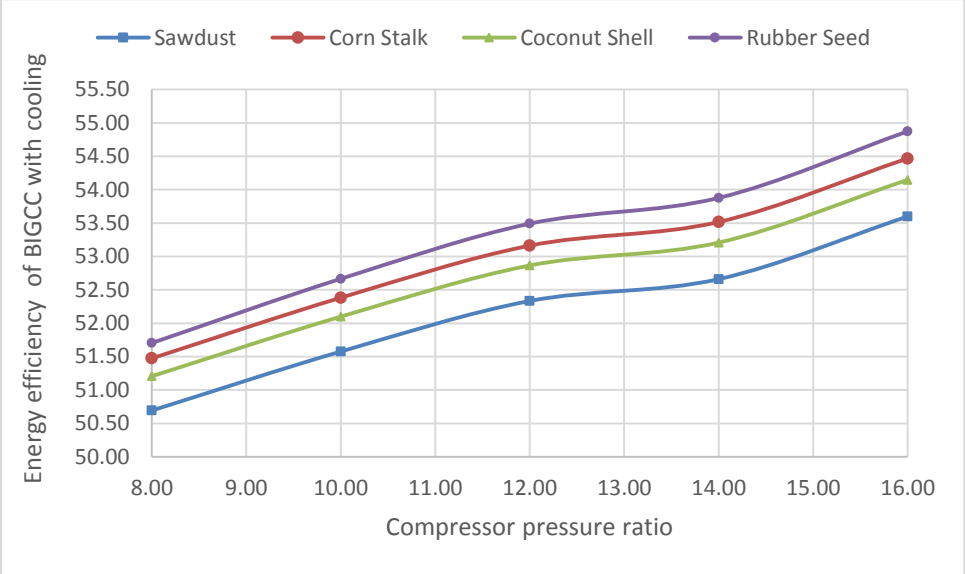

Figure 30: Effect of compressor pressure ratio in energy efficiency of BIGCC with LiBr-H_2O cooling system

The exergy efficiency which is considered to be more perfect than the energy efficiency of the cycle is also examined for the combined cycle and its variation with the compressor pressure ratio is shown in Figure 31. It is found that the exergy efficiency of the combined cycle like its energy efficiency increases with the increase of compressor pressure ratio. The reason for the increase in its exergy efficiency is same as discussed for the trend obtained in Figure 30. Increase in compressor pressure ratio from 8 to 16 results in the small increase of the exergy efficiency of gasifier from 40% to 40.5% in case of rubber seed derived syngas fueled combined cycle. Change in biomass from rubber seed to saw dust increases the exergy efficiency of combined cycle from 40% to 43.5% at the compressor pressure ratio of 8.

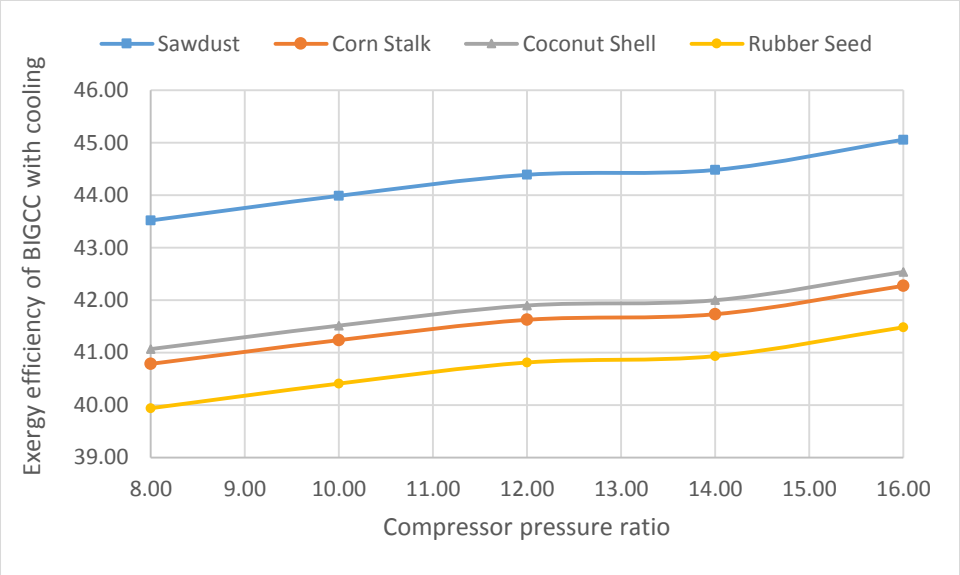

Figure 31: Effect of compressor pressure ratio in exergy efficiency of BIGCC with LiBr-H_2O cooling system

4.4 Effect of Change in Pinch Point Temperature at HRSG

Pinch point temperature difference at the HRSG of BIGCC was taken as another operating variable of the system and its effect on its energy efficiency was investigated which is shown in Figure 32. It is observed that increase in pinch point from 10 to 50 causes a decrease in the energy efficiency of corn stalk fueled BIGCC from 54.2% to 49.3%. Change in biomass material show a little impact on the energy efficiency of BIGCC at a given pinch point temperature. Since the exhaust gas temperature at the exit of HRSG increases with the increase of pinch point temperature which results in the reduced production of steam in HRSG and hence the reduced steam turbine output which in turn decrease the efficiency of BIGCC. A sharp reduction in the efficiency of

BIGCC with the increase in pinch point is observed due to more heat loss at the exit of HRSG.

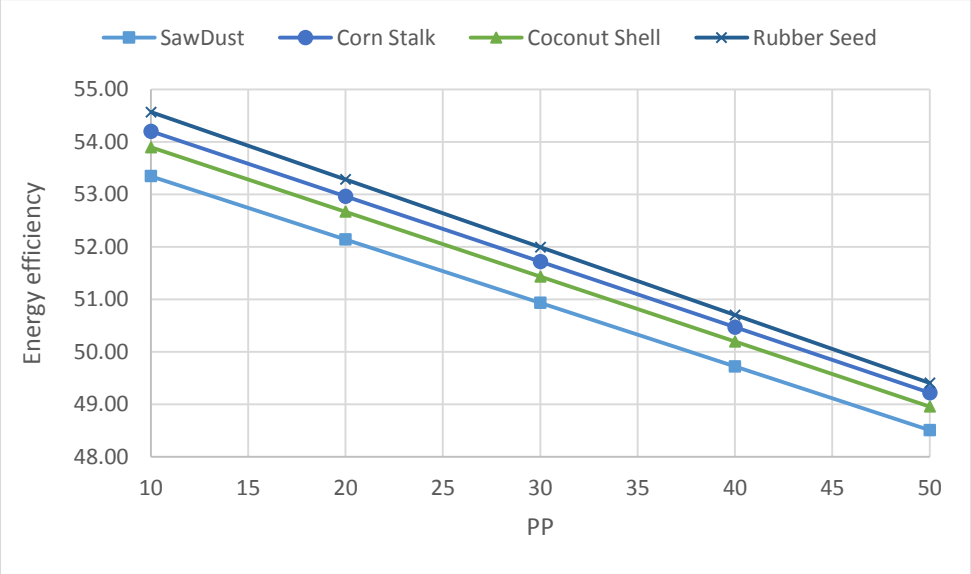

Figure 32: Effect of pinch point temperature at HRSG on the energy efficiency of BIGCC

The effect of pinch point temperature on the exergy efficiency of BIGCC is also examined and shown in Figure 33 where it is found that the exergy efficiency decreases with the increase in pinch point. This is due to the reasons explained for Figure 32. It is further seen that the decrease in exergy efficiency is not so steep as the energy efficiency which is due to the fact that the amount of exergy associated with steam produced at HRSG is considerably less than its energy quantity. The change in biomass from rubber seed to saw dust show a change in exergy efficiency of BIGCC from 40.8% to 44.5% at the pinch point of 10. The change in biomass material on exergy efficiency of BIGCC is almost equally pronounced for all selected values of pinch point temperature.

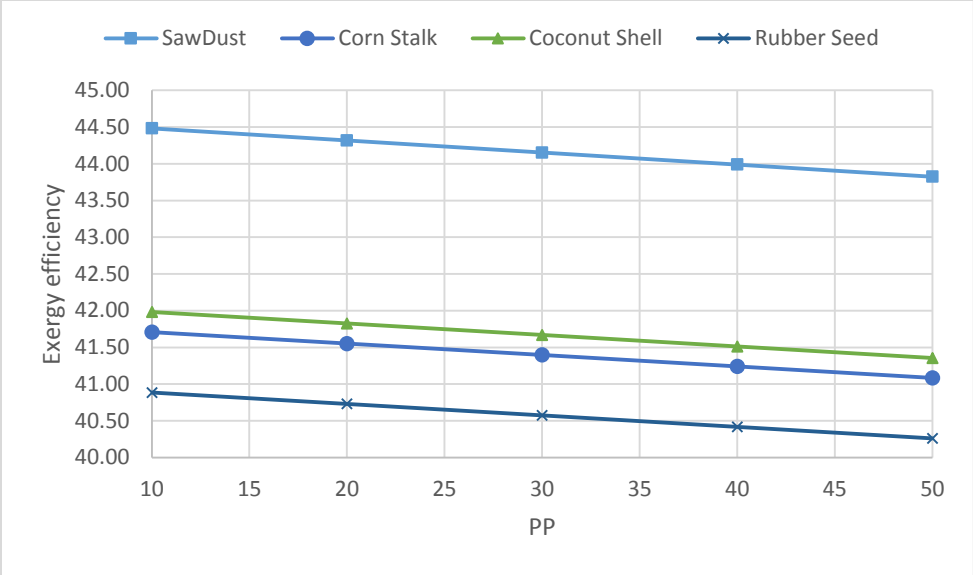

Figure 33: Effect of pinch point temperature at HRSG on the exergy efficiency of BIGCC

The effect of a change in pinch point temperature on the energy efficiency of combined cycle is also shown and displayed in Figure 34 where it is seen that energy efficiency of combined BIGCC-VAR cycle decreases with the increase of pinch point. This is due to the reason that increase in pinch point causes a reduction in the production of steam at HRSG due to the increase in temperature of flue gasses at the exit of HRSG. The reduced steam flow rate to the turbine gives a lesser power output and hence the efficiency. The increase in pinch point increases the temperature of gasses goes out from the generator of VAR to the ambient which also contributes towards the decrease in the efficiency of combined cycle. The change in biomass material also has an impact on the efficiency of combined cycle.

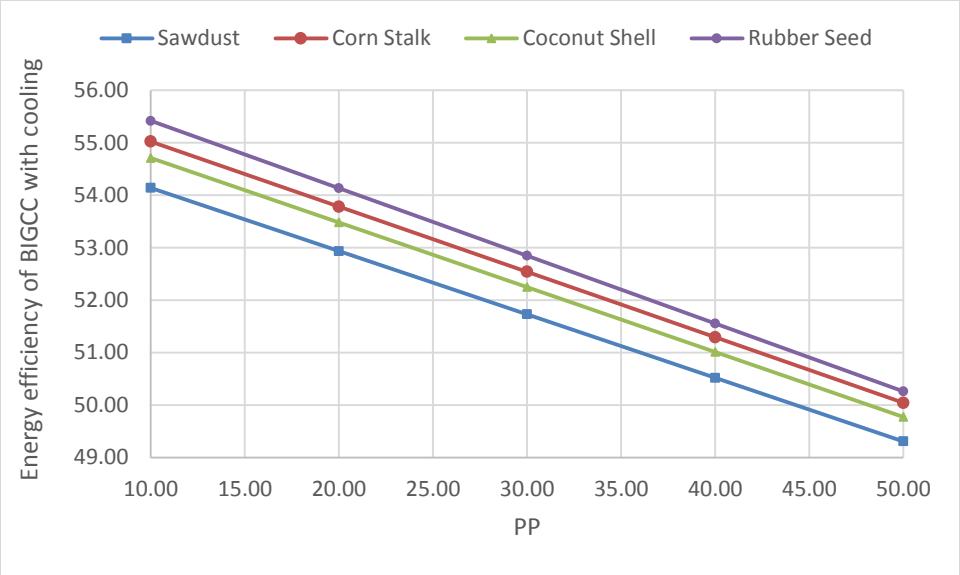

Figure 34: Effect of pinch point in HRSG in energy efficiency of BIGCC with LiBr-H_2O cooling system

The exergy efficiency of the combined BIGCC-VAR system was examined for the change in pinch point temperature at HRSG and shown in Figure 35 where it seen that the exergy efficiency of combined cycle also decreases with the increase in pinch point temperature. It is further noticed that increase in the energy efficiency of combined cycle is greater than the decrease in the exergy efficiency of the combined cycle at a given pinch point temperature for all biomasses. This is due to the fact that the exergy destroyed due to heat transfer a finite temperature difference at HRSG is considerably less than the heat transfer itself which results in the decrease of the exergy of steam going to turbine. The effect of change in biomass material is equally pronounced for the change of exergy efficiency of combined cycle at all pinch point temperatures selected for the analysis.

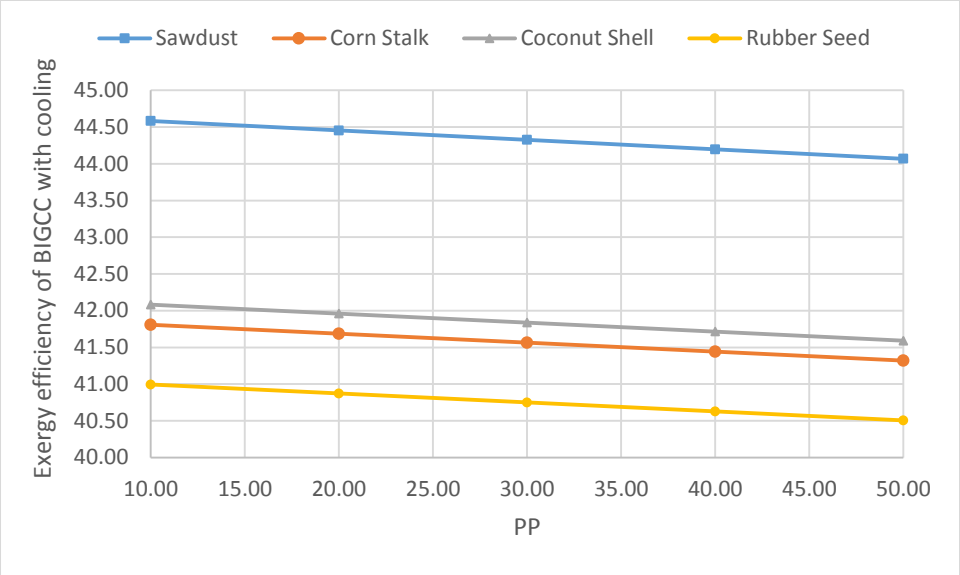

Figure 35: Effect of pinch point of HRSG in exergy efficiency of BIGCC with LiBr-H_2O cooling system

4.5 Exergy Efficiency of Every Component

Exergy efficiency of a component which is the measure of its true thermodynamic performance is also investigated and the exergy efficiency of each component of the proposed BIGCC is shown in Figure 36. It is found that largest exergy destruction happens at the gasifier which is due to the occurrence of the simultaneous reactions of partial oxidation and reduction at the gasifier. The occurrence of chemical reaction in the energy conversion system is the biggest source of exergy destruction from a second law point of view. Due to this reason, maximum exergy destroyed at the gasifier and second largest exergy destruction occurs in the combustion chamber of BIGCC which resulted in the exergy efficiency of gasifier around 40% and of combustion chamber around 80%, respectively. In other components of BIGCC where the invariable chemical composition of the working substance exists during the energy conversion from given one to the desired one, a very high value of exergy efficiency is observed because only changes in physical

exergy of the working fluid will take place during these processes. Figure 36 reveals that almost 100% is the exergy efficiency of compressor gas turbine, and steam condenser. This is due to the fact that the phase of working fluid is gaseous throughout and compression/expansion approaches to isentropic. Due to the existence of small temperature difference at the HRSG and steam turbine which carries the little entropy generation some exergy is destroyed in HRSG and steam turbine that leads to the exergy efficiency of these components less than 100%. The change in biomass material has very little impact on the exergy efficiency of every component of BIGCC.

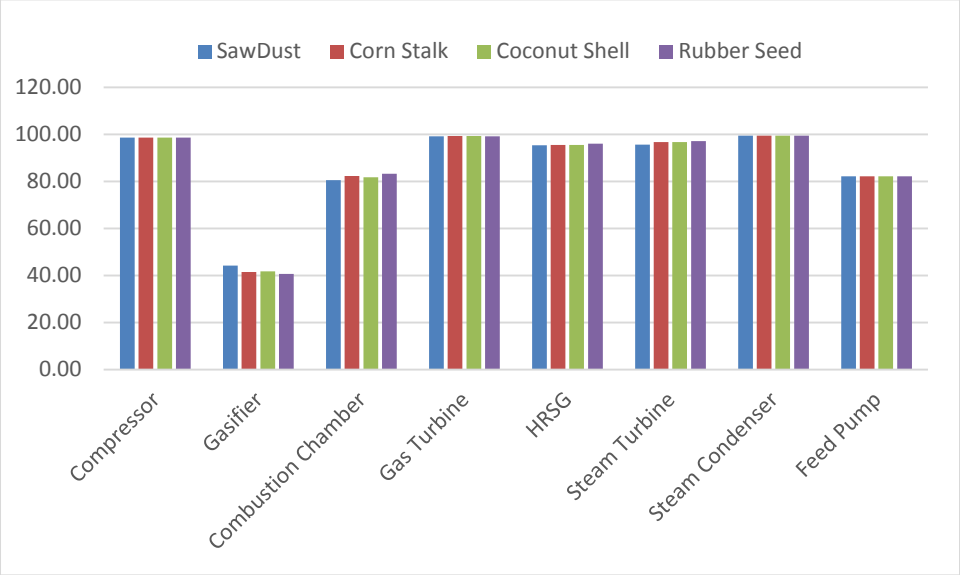

Figure 36: Exergy efficiency of the components of the BIGCC at mean operating condition

Exergy efficiency of the components of bottoming cycle were also computed after taking into accounts only the physical exergy which is displayed in Figure 37 where it is found that the exergy efficiency of the VAR components is comparable to the components of BIGCC other than the gasifier and combustion chamber. Results show the exergy

efficiency of generator around 70%, solution heat exchanger 84%, absorber 90%, condenser around 95%, evaporator close to 100%, and solution pump also close to 100%. The reason for having a less exergy efficiency of generator is the entropy generation due to splitting of solution into the refrigerant and absorbent as well as the entropy generation due to the heat transfer at a finite temperature difference. At solution heat exchanger, a considerable temperature difference exists that leads to higher entropy generation via heat transfer and a lesser exergy efficiency. Mixing of the refrigerant and absorbent and finite temperature difference heat transfer at the evaporator leads to a considerable amount of entropy generation and hence a lesser exergy efficiency of the component concerned. Since the amount of exergy associated with the cooling effect at the evaporator and the rise in pressure at the solution pump are small therefore, the exergy efficiency of these two components approaches to 100%.

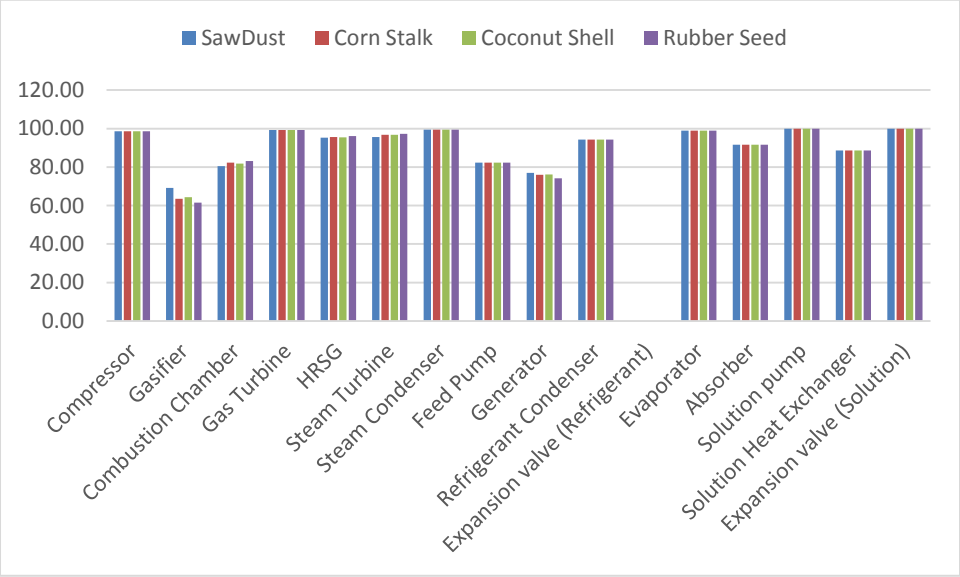

Figure 37: Exergy efficiency of each component with physical exergy in VAR

The most interesting part of the results obtained is the evaluation of the exergy efficiency of the component of the combined BIGCC-VAR cycle with the incorporation of the chemical exergy of LiBr-H2O mixture. The exergy efficiency of each component of the combined cycle is computed at the mean operating conditions of the cycle and shown in Figure 38. Comparison of Figure 37 and 38 clearly show that the exergy efficiency of the components of VAR cycle reflects differently after the inclusion of the chemical exergy of the solution. The exergy efficiency of the generator, absorber, and solution heat exchanger changes from 70% to 95%, 90% to 93.78%, and 84% to 99%, respectively. This significant deviation in the values of the exergy efficiency of the key components of the VAR reveals the importance of chemical exergy inclusion in the computation of results. Therefore the exergy analysis done alone with the incorporation of physical exergy is inadequate and hence the inclusion of chemical exergy is desired for the assessment of the true exergetic performance of the combined power and cooling cycle.

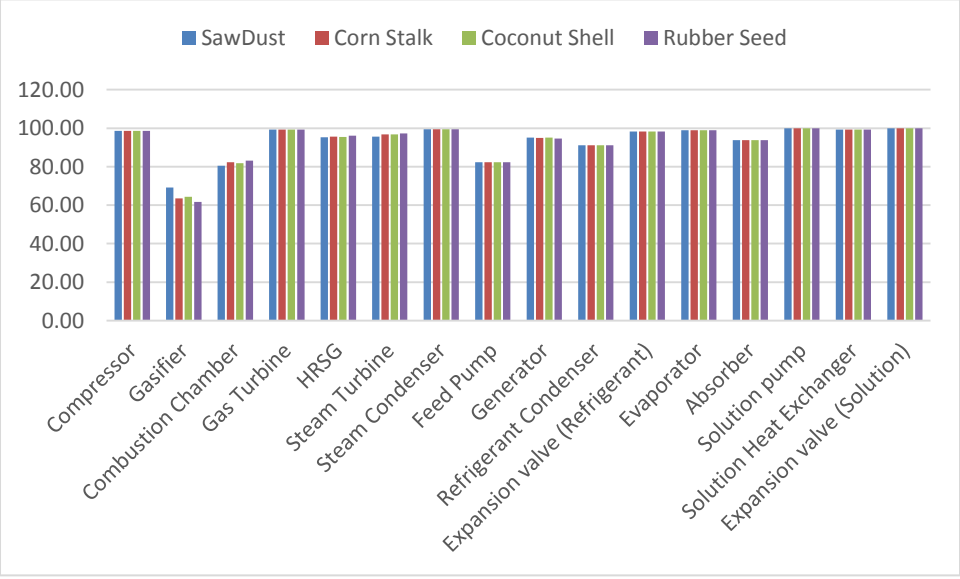

Figure 38: Exergy efficiency of every component with physical and chemical exergy in VAR

CHAPTER 5

CONCLUSION AND RECOMMENDATIONS

The model developed in the current study was tested to compute the syngas composition and the energetic and exergetic performance of the gasifier, BIGCC and BIGCC-VAR were evaluated. Based on the research work carried out and results obtained, following may be considered as the concluding remarks of the present study:

1. The energy efficiency of gasifier decreases from 44% to 28% and its exergy decreases from 52% to 34% when the gasification equivalence ratio increases from 0.3 to 0.6.

2. The LHV of syngas also affected considerably with the GER and it is seen that increase in GER from 0.3 to 0.6 decreases the LHV from 17 MJ to 12.5 MJ for saw dust gasification.

3. The change in biomass material has a little impact on the energetic and exergetic performance of the gasifier and it shows the same trend for all parameters for all selected biomasses with little deviation.

4. The energy and exergy efficiency of the gasifier varies from 43% to 32% and 45% to 42.9%, respectively when the SBR increases from 0.5 to 1.2.

5. The energy and exergy efficiency of biomass integrated combined cycle (BIGCC) varies from 50.3% to 52.2% and from 42.9% to 45.4%, respectively when the SBR changes from 0.5 to 1.2.

6. Change in compressor pressure ratio from 8 to 16 raises the energy efficiency of BIGCC from 49.9% to 52.2% and exergy efficiency from 43.4% to 44.9%, respectively.

7. Change in pinch point temperature at HRSG from 10K to 50K decreases the energy efficiency of BIGCC from 53.5% to 48.5% and exergy efficiency from 44.5% to 43.75%, respectively.

8. Integration of VAR system with the BIGCC give rise an improvement in both the energy and exergy efficiency of the cycle and it is seen that at SBR of 0.5 for saw dust biomass the energy efficiency of the BIGCC increased from 50.3% to 51.5% and its exergy efficiency increased from 42.9% to 43% when it is integrated with VAR. The increase in exergy efficiency is lesser than energy efficiency for obvious reasons.

9. The exergy destruction in the components of BIGCC-VAR was also computed in order to rank the cycle components from a performance point of view. The exergy efficiency of each component of the combined cycle was evaluated and this follow the ascending order of gasifier 44.2%, generator 75.98%, combustion chamber 80.55%, feed water pump 82.23%, solution heat exchanger 88.83%, absorber 91.65%, HRSG 95.33%, refrigerant condenser 94.29%, steam turbine 95.65%. The exergy efficiency of the other combined cycle components approaches to 100%.

This figure of results reveals when only physical exergy of LiBr-H_2O taking into accounts.

10. Inclusion of chemical exergy in the exergetic analysis of the combined cycle along with the physical exergy changes the percentage of the exergy efficiency of cycle components and follow the given ascending order gasifier 44.24%, combustion chamber 80.55%, feed water pump 82.23%, refrigerant condenser 91.11%, absorber 93.78%, generator 95.19%, HRSG 95.33%, steam turbine 95.65%.

11. The efficiency of BIGCC along with VAR is found to be optimum at GER ranges from 0.35 to 0.4, SBR from 0.85 to 1, compressor pressure ratio of 16 and pinch point of HRSG at 10 K for different biomasses.

The thermo-economic analysis which combines the laws of thermodynamics with the basic principles of economics is recommended as a future scope of the present study through which both the performance assessment and cost evaluation of the components and the concerned cycle can be made and hence the thermodynamic limits and the economic viability of the proposed cycle can be predicted.

References

[1] "World Energy Resources 2016." [Online]. Available: https://www.worldenergy.org/publications/2016/world-energy-resources-2016/.

[2] "Yard waste, Chips and Woods on Pinterest." [Online]. Available: https://www.pinterest.com/pin/196188127486855025/.

[3] R. Warnecke, "Gasification of biomass: comparison of fixed bed and fluidized bed gasifier," Biomass and Bioenergy, vol. 18, no. 6, pp. 489–497, 2000.

[4] A. Franco and N. Giannini, "Perspectives for the use of biomass as fuel in combined cycle power plants," Int. J. Therm. Sci., vol. 44, no. 2, pp. 163–177, 2005.

[5] T. Hasegawa and T. Tamaru, "Gas turbine combustion technology reducing both Fuel-NO_x and Thermal-NO_x emissions for oxygen-blown IGCC with Hot/Dry synthetic gas cleanup," J. Eng. Gas Turbines Power, vol. 129, no. 2, p. 358, 2007.

[6] "Integrated gasification combined-cycle | ClimateTechWiki." [Online]. Available: http://www.climatetechwiki.org/technology/igcc.

[7] C. Higman and M. van der. Burgt, "Gasification," Gulf Professional Pub./Elsevier Science, 2008.

[8] P. Mathieu and R. Dubuisson, "Performance analysis of a biomass gasifier," Energy Convers. Manag., vol. 43, no. 9, pp. 1291–1299, 2002.

[9] R. Brunner, Handbook of solid waste management. McGraw-Hill,New York, 2002.

[10] T. Abbas, P. G. Costen, and F. C. Lockwood, "Solid fuel utilization: From coal to biomass," Symp. Combust., vol. 26, no. 2, pp. 3041–3058, 1996.

[11] L. Kimes, "Biomass conversion: Emerging technologies, feedstocks, and products," Sustain. Program, Off. Res. Dev. US Environ. Prot. Agency, 2007.

[12] F. Delattin, J. De Ruyck, and S. Bram, "Detailed study of the impact of co-utilization of biomass in a natural gas combined cycle power plant through perturbation analysis," Appl. Energy, vol. 86, no. 5, pp. 622–629, 2009.

[13] E. E. Hughes and D. A. Tillman, "Biomass cofiring: status and prospects 1996," Fuel Process. Technol., vol. 54, no. 1, pp. 127–142, 1998.

[14] A. V. Bridgwater, "The technical and economic feasibility of biomass gasification for power generation," Fuel, vol. 74, no. 5, pp. 631–653, 1995.

[15] D. . McIlveen-Wright, B. . Williams, and J. . McMullan, "Wood gasification integrated with fuel cells," Renew. Energy, vol. 19, no. 1, pp. 223–228, 2000.

[16] Mark A. Paisley and Mike J. Welch, "Biomass gasification combined cycle

opportunities using the future energy SilvaGas® gasifier coupled to Alstom's industrial gas turbines," ASME Turbo Expo, vol. 1, pp. 211–217, 2003.

[17] T. Savola, "Simulation and optimisation of power production in biomass-fuelled small-scale CHP plants.," Helsinki Univ. Technol., 2005.

[18] K. M. Margaret and L. S. Pamela, "Life cycle assessment comparisons of electricity from biomass, coal, and natural nas," Modeling the Environment. 2002.

[19] S. Panigrahi, A. K. Dalai, S. T. Chaudhari, and N. N. Bakhshi, "Synthesis gas production from steam gasification of biomass-derived oil," Energy & Fuels, vol. 17, no. 3, pp. 637–642, 2003.

[20] S. T. Chaudhari, S. K. Bej, N. N. Bakhshi, and A. K. Dalai, "Steam gasification of biomass-derived char for the production of carbon monoxide-rich synthesis gas," Energy and Fuels, vol. 15, no. 3, pp. 736–742, 2001.

[21] S. T. Chaudhari, A. K. Dalai, and N. N. Bakhshi, "Production of hydrogen and/or syngas (H_2 + CO) via steam gasification of biomass-derived chars," Energy and Fuels, vol. 17, no. 4, pp. 1062–1067, 2003.

[22] Z. Q. Wang, N. J. Zhou, J. Guo, and X. Y. Wang, "Fluid selection and parametric optimization of organic Rankine cycle using low temperature waste heat," Energy, vol. 40, no. 1, pp. 107–115, 2012.

[23] X. L. Yin, C. Z. Wu, S. P. Zheng, and Y. Chen, "Design and operation of a CFB gasification and power generation system for rice husk," Biomass and Bioenergy, vol. 23, no. 3, pp. 181–187, 2002.

[24] T. Srinivas, B. V. Reddy, and a. V. S. S. K. S. Gupta, "Thermal performance prediction of a biomass based integrated gasification combined cycle plant," J. Energy Resour. Technol., vol. 134, no. 2, p. 21002, 2012.

[25] Z. A. B. Z. Alauddin, P. Lahijani, M. Mohammadi, and A. R. Mohamed, "Gasification of lignocellulosic biomass in fluidized beds for renewable energy development: A review," Renew. Sustain. Energy Rev., vol. 14, no. 9, pp. 2852–2862, 2010.

[26] S. Kaiser, K. Weigl, A. Friedl, and H. Hofbauer, "Process product gas flue gas biomass steam air," pp. 0–4.

[27] Y. Cao, Y. Wang, J. T. Riley, and W.-P. Pan, "A novel biomass air gasification process for producing tar-free higher heating value fuel gas," Fuel Process. Technol., vol. 87, no. 4, pp. 343–353, 2006.

[28] J. Delgado, M. P. Aznar, and J. Corella, "Biomass gasification with steam in fluidized bed: effectiveness of CaO, MgO, and CaO-MgO for hot raw gas cleaning," Ind. Eng. Chem. Res., vol. 36, pp. 1535–1543, 1997.

[29] I. Narvaez, A. Orıo, M. P. Aznar, and J. Corella, "Biomass gasification with air in

an atmospheric bubbling fluidized bed . Effect of six operational variables on the quality of syngas," Ind. Eng. Chem. Res., vol. 35, no. 95, pp. 2110–2120, 1996.

[30] P. McKendry, "Energy production from biomass (part 3): Gasification technologies," Bioresour. Technol., vol. 83, no. 1, pp. 55–63, 2002.

[31] X. T. Li, J. R. Grace, C. J. Lim, A. P. Watkinson, H. P. Chen, and J. R. Kim, "Biomass gasification in a circulating fluidized bed," Biomass and Bioenergy, vol. 26, no. 2, pp. 171–193, 2004.

[32] P. Lv, Z. Yuan, C. Wu, L. Ma, Y. Chen, and N. Tsubaki, "Bio-syngas production from biomass catalytic gasification," Energy Convers. Manag., vol. 48, no. 4, pp. 1132–1139, 2007.

[33] M. Campoy, A. Gómez-Barea, F. B. Vidal, and P. Ollero, "Air-steam gasification of biomass in a fluidised bed: Process optimisation by enriched air," Fuel Process. Technol., vol. 90, no. 5, pp. 677–685, 2009.

[34] A. Gómez-Barea and B. Leckner, "Estimation of gas composition and char conversion in a fluidized bed biomass gasifier," Fuel, vol. 107, pp. 419–431, 2013.

[35] C. R. Coronado, J. T. Yoshioka, and J. L. Silveira, "Electricity, hot water and cold water production from biomass. Energetic and economical analysis of the compact system of cogeneration run with woodgas from a small downdraft gasifier," Renew. Energy, vol. 36, no. 6, pp. 1861–1868, 2011.

[36] A. Shah, R. Srinivasan, S. D. Filip To, and E. P. Columbus, "Performance and emissions of a spark-ignited engine driven generator on biomass based syngas," Bioresour. Technol., vol. 101, no. 12, pp. 4656–4661, 2010.

[37] U. Azimov, E. Tomita, N. Kawahara, and Y. Harada, "Effect of syngas composition on combustion and exhaust emission characteristics in a pilot-ignited dual-fuel engine operated in PREMIER combustion mode," Int. J. Hydrogen Energy, vol. 36, no. 18, pp. 11985–11996, 2011.

[38] R. Chacartegui, M. Torres, D. Sánchez, F. Jiménez, A. Muñoz, and T. Sánchez, "Analysis of main gaseous emissions of heavy duty gas turbines burning several syngas fuels," Fuel Process. Technol., vol. 92, no. 2, pp. 213–220, 2011.

[39] R. L. Fagbenle, a. B. C. Oguaka, and O. T. Olakoyejo, "A thermodynamic analysis of a biogas-fired integrated gasification steam injected gas turbine (BIG/STIG) plant," Appl. Therm. Eng., vol. 27, no. 13, pp. 2220–2225, 2007.

[40] M. J. De Kam, R. Vance Morey, and D. G. Tiffany, "Biomass integrated gasification combined cycle for heat and power at ethanol plants," Energy Convers. Manag., vol. 50, no. 7, pp. 1682–1690, 2009.

[41] C. Wu, X. Yin, L. Ma, Z. Zhou, and H. Chen, "Operational characteristics of a 1.2-MW biomass gasification and power generation plant," Biotechnol. Adv., vol. 27, no. 5, pp. 588–592, 2009.

[42] H. H. Finckh and H. Pfost, “Development potential of combined-cycle (GUD) power plants with and without supplementary firing,” J. Eng. Gas Turbines Power, vol. 114, no. 4, p. 653, 1992.

[43] T. Srinivas, a. V. S. S. K. S. Gupta, and B. V. Reddy, “Thermodynamic equilibrium model and exergy analysis of a biomass gasifier,” J. Energy Resour. Technol., vol. 131, no. September 2009, p. 31801, 2009.

[44] P. Mondal, K. Mondal, and S. Ghosh, “Bio- gasification based distributed power generation system employing indirectly heated GT and supercritical ORC : Energetic and exergetic performance assessment,” vol. 5, no. 3, 2015.

[45] S. HEM, P. W, and van S. WPM, “Thermal conversion of biomass into secondary products, the case of gasification and pyrolysis,” in Proceeding of twelfth European conference on biomass for energy, industry and climate protection, June 17e21, 2002.

[46] M. Puig-Arnavat, J. C. Bruno, and A. Coronas, “Review and analysis of biomass gasification models,” Renew. Sustain. Energy Rev., vol. 14, no. 9, pp. 2841–2851, 2010.

[47] Z. A. Zainal, R. Ali, C. H. Lean, and K. N. Seetharamu, “Prediction of performance of a downdraft gasifier using equilibrium modeling for different biomass materials,” Energy Convers. Manag., vol. 42, no. 12, pp. 1499–1515, 2001.

[48] M. J. Prins, K. J. Ptasinski, and F. J. J. G. Janssen, “Thermodynamics of gas-char reactions: first and second law analysis,” Chem. Eng. Sci., vol. 58, no. 3–6, pp. 1003–1011, 2003.

[49] S. Jarungthammachote and a. Dutta, “Thermodynamic equilibrium model and second law analysis of a downdraft waste gasifier,” Energy, vol. 32, no. 9, pp. 1660–1669, 2007.

[50] M. Venkata Ramanan, E. Lakshmanan, R. Sethumadhavan, and S. Renganarayanan, “Performance prediction and validation of equilibrium modeling for gasification of cashew nut shell char,” Brazilian J. Chem. Eng., vol. 25, no. 3, pp. 585–601, 2008.

[51] H.-J. Huang and S. Ramaswamy, “Modeling biomass gasification using thermodynamic equilibrium approach,” Appl. Biochem. Biotechnol., vol. 154, no. 1–3, pp. 14–25, 2009.

[52] E. Azzone, M. Morini, and M. Pinelli, “Development of an equilibrium model for the simulation of thermochemical gasification and application to agricultural residues,” Renew. Energy, vol. 46, pp. 248–254, 2012.

[53] S. Rupesh, C. Muraleedharan, and P. Arun, “Analysis of hydrogen generation through thermochemical gasification of coconut shell using thermodynamic equilibrium model considering char and tar,” Int. Sch. Res. Not., vol. 2014, pp. 1–9, 2014.

[54] S. Rupesh, C. Muraleedharan, and P. Arun, “A comparative study on gaseous fuel generation capability of biomass materials by thermo-chemical gasification using stoichiometric quasi-steady-state model,” Int. J. Energy Environ. Eng., vol. 6, no. 4, pp. 375–384, 2015.

[55] K. H. Kim and K. Kim, “Exergy analysis of overspray process in gas turbine systems,” Energies, vol. 5, no. 12, pp. 2745–2758, Jul. 2012.

[56] M. Parvez and A. Khaliq, “Exergy analysis of a syngas fuelled cogeneration cycle for combined production of power and refrigeration,” Int. J. Exergy, vol. 14, no. 1, p. 1, 2014.

[57] Y. Kalinci, A. Hepbasli, and I. Dincer, “Exergoeconomic analysis of hydrogen production from biomass gasification,” Int. J. Hydrogen Energy, vol. 37, no. 21, pp. 16402–16411, 2012.

[58] Y. Il Lim and U. Do Lee, “Quasi-equilibrium thermodynamic model with empirical equations for air-steam biomass gasification in fluidized-beds,” Fuel Process. Technol., vol. 128, pp. 199–210, 2014.

[59] T. H. Jayah, L. Aye, R. J. Fuller, and D. F. Stewart, “Computer simulation of a downdraft wood gasifier for tea drying,” Biomass and Bioenergy, vol. 25, no. 4, pp. 459–469, 2003.

[60] C. R. Altafini, P. R. Wander, and R. M. Barreto, “Prediction of the working parameters of a wood waste gasifier through an equilibrium model,” Energy Convers. Manag., vol. 44, no. 17, pp. 2763–2777, 2003.

[61] R. Karamarkovic and V. Karamarkovic, “Energy and exergy analysis of biomass gasification at different temperatures,” Energy, vol. 35, no. 2, pp. 537–549, 2010.

[62] T. J. Kotas, The Exergy Method of Thermal Plant Analysis. Malabar: Krieger Publishing, 1995.

[63] A. Khaliq, “Energetic and exergetic performance evaluation of a gas turbine – powered cogeneration system using reverse brayton refrigeration cycle for inlet air cooling,”ASME, pp. 1–11, 2013.

[64] T. D. B. Nguyen, S. I. Ngo, Y. Il Lim, J. W. Lee, U. Do Lee, and B. H. Song, “Three-stage steady-state model for biomass gasification in a dual circulating fluidized-bed,” Energy Convers. Manag., vol. 54, no. 1, pp. 100–112, 2012.

[65] P. Ahmadi, I. Dincer, and M. A. Rosen, “Multi-objective optimization of a novel solar-based multigeneration energy system,” Sol. Energy, vol. 108, pp. 576–591, 2014.

[66] A. Khaliq, “Performance analysis of a waste-heat-powered thermodynamic cycle for multieffect refrigeration,” Int. J. Energy Res., vol. 39, no. 4, pp. 529–542, Mar. 2015.

[67] T. K. Gogoi, “Estimation of operating parameters of a Water–LiBr vapor Absorption refrigeration system through inverse analysis,” J. Energy Resour. Technol., vol. 138, no. 2, p. 22002, 2015.

[68] J. Pátek and J. Klomfar, “A computationally effective formulation of the thermodynamic properties of LiBr–H2O solutions from 273 to 500K over full composition range,” Int. J. Refrig., vol. 29, no. 4, pp. 566–578, 2006.

[69] M. M. M. Talbi and B. Agnew, “Exergy analysis: an absorption refrigerator using lithium bromide and water as the working fluids,” Appl. Therm. Eng., vol. 20, no. 7, pp. 619–630, 2000.

[70] R. Palacios-Bereche, R. Gonzales, and S. A. Nebra, “Exergy calculation of lithium bromide-water solution and its application in the exergetic evaluation of absorption refrigeration systems LiBr-H2O,” Int. J. Energy Res., vol. 36, no. 2, pp. 166–181, Feb. 2012.

[71] D. S. Kim and C. a. Infante Ferreira, “A Gibbs energy equation for LiBr aqueous solutions,” Int. J. Refrig., vol. 29, no. 1, pp. 36–46, 2006.

Vitae

Name	: Robhul Miah
Nationality	: Bangladeshi
Date of Birth	:6/30/1987
Email	: robhul05me@yahoo.com
Address	: 50/5, Khulna Polytechnic College Road, Bangladesh
Academic Background	: Masters in Mechanical Engineering (Jan, 2017) King Fahd University of Petroleum and Minerals. Bachelor in Mechanical Engineer (Feb, 2011) Bangladesh University of Engineering and Technology